

SAMPLE LOTTERY: UNSUPERVISED DISCOVERY OF CRITICAL INSTANCES IN RLVR OF LLMs

000
001
002
003
004
005 **Anonymous authors**
006 Paper under double-blind review
007
008
009
010
011
012
013
014
015
016
017
018
019
020
021
022
023
024
025
026
027
028
029
030
031
032
033
034
035
036
037
038
039
040
041
042
043
044
045
046
047
048
049
050
051
052
053

ABSTRACT

Reinforcement Learning with Verifiable Reward (RLVR) has equipped large language models (LLMs) with the capability of reasoning over complicated logical problems through policy optimization. However, conventional methods require complete annotation of the entire dataset and allocate computation uniformly over all samples. We articulate the *lottery sample hypothesis* in policy optimization of LLMs: a large training set contains a small subset that, when trained alone, yields performance comparable to that of the full dataset. This paper therefore explores the following question: *How can we identify these lottery-winning samples from the original dataset without access to answers?* Unlike prior efforts that analyze the effect of different samples in the training set with complete annotation, this paper focuses on the unsupervised discovery of critical instances for LLM reasoning and proposes a novel framework termed Complementary Conformal Selection (CONST). Specifically, CONST evaluates the importance of samples by considering two complementary components: *procedural volatility* and *outcome volatility*. Procedural volatility measures the potential variations during the LLM’s reasoning process, while outcome volatility captures inconsistencies in the final answer. Subsequently, conformal prediction is used to obtain a prediction set whose cardinality serves as the criterion for selecting the lottery-winning samples for annotation. We also provide a theoretical analysis, showing that CONST can effectively approximate the optimal policy. Extensive experiments on various LLMs across different datasets demonstrate the effectiveness of CONST. The code is available at <https://anonymous.4open.science/r/CONST-359D>.

1 INTRODUCTION

Reinforcement learning (RL) has recently become an essential tool for post-training of large language models (LLMs) (Anil et al., 2023; OpenAI, 2024; 2025; Guo et al., 2025; Du et al., 2025). Policy optimization algorithms (Schulman et al., 2017; Shao et al., 2024) have significantly enhanced the logical reasoning capabilities of LLMs (DeepMind, 2024; Wang et al., 2025a; Ren et al., 2025). For logical problems, directly verifiable answers provide straightforward rewards for reinforcement learning, enabling effective outcome supervision of LLMs. This approach, known as reinforcement learning with verifiable reward (RLVR) (Gao et al., 2024; Lambert et al., 2024), is commonly implemented using algorithms such as Group Relative Policy Optimization (GRPO) (Shao et al., 2024) and its variants (Liu et al., 2025d; Chen et al., 2025; Pang & Jin, 2025; Zhang et al., 2025b).

Despite the significant improvement, conventional approaches (Hao et al., 2025; Wu et al., 2025; Di et al., 2025) demand full annotation over the entire dataset for verification, and often allocate computation resources uniformly across the full dataset. Nevertheless, some recent studies in RLVR of LLMs (Chen et al., 2025; Wang et al., 2025c; Vanlioglu, 2025) and many prior works on the more general field of data subset selection and valuation (Paul et al., 2021; Das et al., 2021b; Guo et al., 2022; Das et al., 2024) suggest that the instances in the training set are not equally important, and that training on a small subset may also lead to satisfactory results (Wang et al., 2025c). Based on these findings, we articulate the *lottery sample hypothesis* in RLVR of LLMs:

A large training set for RLVR on LLMs contains a small subset that, when trained alone, can achieve performance comparable to that of the full dataset.

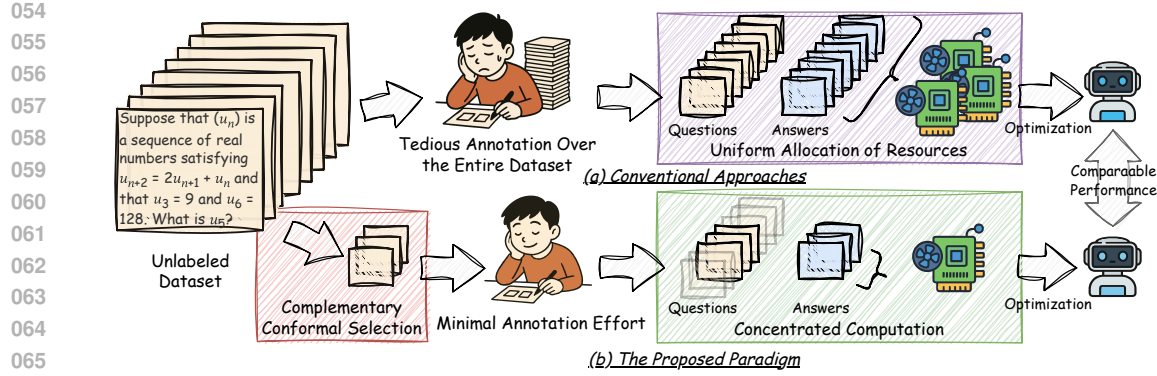


Figure 1: Conventional approaches require tedious full annotation over the entire dataset and allocate computation resources uniformly across the training set. By comparison, this work selects lottery-winning samples from the training set in an unsupervised manner, and then optimizes the model using these critical instances only, achieving comparable performance.

With this hypothesis, it is possible to break conventional approaches from two aspects (as illustrated in Figure 1): (i) full annotation of the dataset is no longer required, and ground truth answers of several lottery-winning samples are sufficient; (ii) computation can be concentrated on several critical instances. Therefore, this paper explores a central question of this new paradigm:

How can we find the critical instances (the lottery-winning samples) for RLVR on LLMs from the original training set without annotation?

To answer this question, this paper proposes a novel framework named Complementary Conformal Selection (CONST) for the unsupervised discovery of critical instances in the training set. CONST evaluates the value of each instance from two complementary perspectives: *procedural volatility* and *outcome volatility*. Procedural volatility assesses potential variations in reasoning chains by examining how different segments of reasoning affect the final answer. Outcome volatility measures inconsistencies in the final answers produced by different reasoning paths. Both yield multisets (*i.e.*, sets that allow duplicating elements) of results, which are then merged and fed into a conformal prediction module. The conformal prediction produces a prediction set, whose cardinality is used as the criterion for selecting lottery-winning samples. A theoretical analysis is also provided demonstrating that CONST can effectively approximate the optimal policy. We conduct extensive experiments across datasets with various LLMs, showing that CONST outperforms various baselines and enables comparable performance with $< 0.5\%$ of the samples. Our contribution is summarized as follows:

- ① **New Perspective:** We present a probabilistic perspective for the unsupervised identification of critical instances in the full dataset for further annotation and RLVR optimization on LLMs, enabling an annotation-minimal, data-efficient and performance-competitive optimization procedure compared with training on the entire fully annotated dataset.
- ② **Novel Methodology with Theoretical Analysis:** We propose CONST, a probabilistic approach based on conformal prediction that considers both procedural volatility and outcome volatility in LLM reasoning, to select lottery-winning samples for annotation and optimization. Notably, we provide a rigorous theoretical analysis of CONST demonstrating that it can effectively approximate the optimal policy parameter setup under the lottery sample hypothesis.
- ③ **Empirical Validation:** We conduct extensive experiments across four mathematical datasets on various LLMs against competing baselines, showing that CONST is (1) **annotation-efficient**, achieving similar performance to the full dataset with $< 0.5\%$ of the annotation, (2) **high-performing**, outperforming competitive baselines by 10.97% on average, and (3) **model-agnostic**, showing consistent improvement across three different architectures.

2 PRELIMINARIES

Problem Definition. Given a training set of questions $\mathcal{Q} = \{X_1, X_2, \dots, X_N\}$ from the input space \mathcal{X} , conventional approaches first annotate the dataset with ground truth answers $\mathcal{A} =$

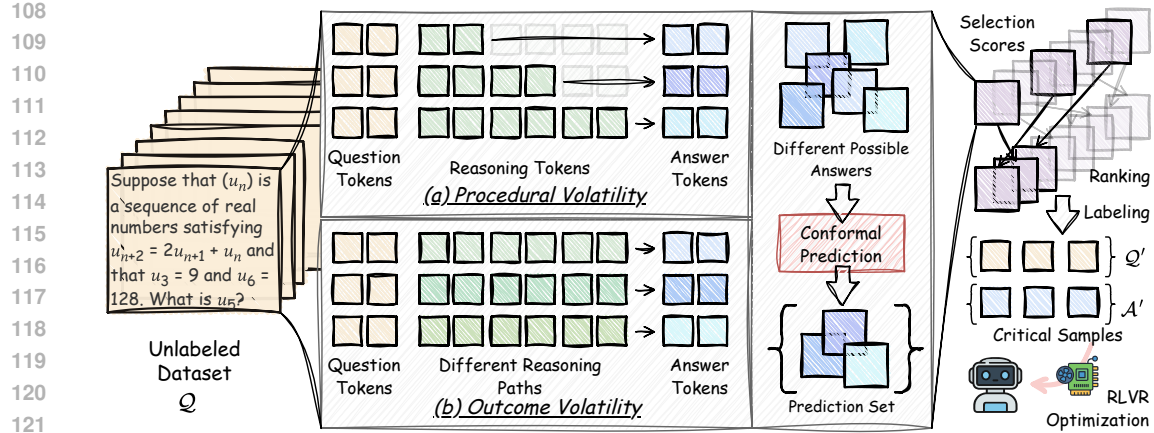


Figure 2: The overall framework of the proposed CONST. CONST selects critical samples via conformal prediction based on both procedural volatility and outcome volatility. The selected samples are then annotated with ground truth answers for standard RLVR optimization on LLMs.

$\{Y_1, Y_2, \dots, Y_N\}$ in the output space \mathcal{Y} , and then optimize the original LLM (*i.e.*, the policy) π_0 with RL algorithms (*e.g.*, GRPO), *i.e.*, $\pi^F = \Phi(\pi_0, \mathcal{Q}, \mathcal{A})$, where π^F is the policy optimized with full data annotation and $\Phi(\cdot, \cdot, \cdot)$ is the optimization process of RLVR. Our goal is to find a subset of \mathcal{Q} with budget b , *i.e.*, $\mathcal{Q}' \subset \mathcal{Q}$ and $|\mathcal{Q}'| = b$, and then annotate the selected data with answers \mathcal{A}' so that the optimized policy $\pi^P = \Phi(\pi_0, \mathcal{Q}', \mathcal{A}')$ achieves comparable performance to π^F .

Reinforcement Learning with Verifiable Reward. During the training process of reinforcement learning with verifiable reward, the LLM generates a list of n outputs $\{O_1, O_2, \dots, O_n\}$ for a question X , and the outputs are verified against the ground truth answer Y to obtain the rewards r_1, r_2, \dots, r_n , where correct answers receive 1 and incorrect ones 0. In the widely adopted group relative policy optimization (Shao et al., 2024; Liu et al., 2025c; Guo et al., 2025), the advantage function of each output O_i is computed as:

$$a_i = \frac{r_i - \text{mean}(\{r_j\}_{j=1}^n)}{\text{std}(\{r_j\}_{j=1}^n)}. \quad (1)$$

With this, the GRPO optimization objective can be formulated as follows:

$$\mathcal{L}_{\text{GRPO}} = \mathbb{E}_{O_i \sim \pi_{\theta'}} \left[-\frac{1}{n} \sum_{i=1}^n \left(\min \left(\frac{\pi_{\theta}(O_i|X)}{\pi_{\theta'}(O_i|X)} a_i, \text{clip} \left(\frac{\pi_{\theta}(O_i|X)}{\pi_{\theta'}(O_i|X)}, 1 - \varepsilon, 1 + \varepsilon \right) a_i \right) \right) \right] + \beta \mathcal{D}_{\text{KL}}(\pi_{\theta} || \pi_0), \quad (2)$$

where π_{θ} is the current policy, $\pi_{\theta'}$ is the old policy, and π_0 is the reference policy.

Conformal Prediction. Conformal prediction (CP) (Vovk et al., 2005; Papadopoulos et al., 2007; Angelopoulos et al., 2023; Barber et al., 2023; Su et al., 2024) is a model-agnostic solution to obtain prediction sets (or intervals in regression tasks) that are mathematically guaranteed to cover the ground truth answer with high probabilities. Concretely, given an input from \mathcal{X} , a prediction from \mathcal{Y} and the prediction model $\pi(Y|X)$, a scoring function $f^{\pi} : \mathcal{X} \times \mathcal{Y} \rightarrow \mathbb{R}$ is defined to quantify the disagreement between the input and the predicted answer. The scoring function is applied to a calibration set $\mathcal{D}^{\text{cal}} = \{(X_i^{\text{cal}}, Y_i^{\text{cal}})\}_{i=1}^m$, which is independently and identically distributed as the dataset under consideration, to obtain the calibration scores $f^{\pi}(X_i^{\text{cal}}, Y_i^{\text{cal}})$, $i = 1, 2, \dots, m$. For a given confidence level $1 - \alpha$, a threshold ρ can be determined by taking the $\frac{\lceil (m+1)(1-\alpha) \rceil}{m}$ quantile of these scores. For a given input $X \in \mathcal{X}$, and the predefined error rate α , the conformal prediction set is guaranteed to cover the correct answer with a probability of $1 - \alpha$, defined as follows:

$$\mathcal{C}_{1-\alpha}(X) = \{Y \mid f^{\pi}(X, Y) \leq \rho\}. \quad (3)$$

162

3 THE PROPOSED CONST

164

3.1 FRAMEWORK OVERVIEW

166 The overall idea of this work is to first select the critical instances \mathcal{Q}' from the training set of ques-
 167 tions \mathcal{Q} using the proposed Complementary Conformal Prediction (**CONST**), then annotate these criti-
 168 cal instances with answers \mathcal{A}' , and finally optimize the LLM using off-the-shelf RLVR algorithms
 169 such as GRPO. The proposed **CONST** evaluates the importance of each instance $X \in \mathcal{Q}$ from two
 170 perspectives: procedural volatility and outcome volatility. Procedural volatility measures how the
 171 final answer to the input question changes when the reasoning paths are truncated at different stages,
 172 while outcome volatility captures the inconsistencies in the final answers produced by different rea-
 173 soning paths. Conformal prediction is then used to obtain a prediction set for each instance, and the
 174 cardinality of these sets serves as the criterion for selecting the critical instances. We illustrate the
 175 overall framework in Figure 2.

176

3.2 PROCEDURAL VOLATILITY

178 Questions important for policy optimization are expected to induce reasoning trajectories of sig-
 179 nificant complexity, as straightforward thinking chains are less likely to substantially enhance the
 180 model’s logical reasoning abilities. Therefore, we propose measuring the volatility in the reasoning
 181 process by truncating the thinking chains at different stages and prompting the LLM to provide the
 182 final answers directly. Simple and straightforward reasoning paths are more likely to yield consistent
 183 answers, whereas complex, intricate ones are more likely to exhibit volatility.

184 Specifically, given a question $X \in \mathcal{Q}$, we first deterministically sample an output, denoted as $O =$
 185 $[t_1, t_2, \dots, t_L; \hat{Y}] = \pi_0(O|X)$, where t_1, t_2, \dots, t_L are tokens of the reasoning path and \hat{Y} is the
 186 predicted answer typically enclosed in special formats like $\backslash\text{box}\{\}$. We truncate the reasoning path
 187 at different stages to obtain a set of truncated reasoning trajectories, defined as follows:

$$188 \quad \mathcal{T}(X) = \{[t_1, t_2, \dots, t_{\lceil \frac{iL}{n_P} \rceil}] \mid i = 1, 2, \dots, n_P\}, \quad (4)$$

190 where n_P is the number of stages. Subsequently, we query the LLM with these truncated trajectories
 191 and ask the model to directly output a single final answer for each truncated trajectory without rea-
 192 soning. Formally, we obtain a multiset (bag)¹ for each sample $X \in \mathcal{Q}$ through response truncation
 193 and LLM re-querying:

$$194 \quad \mathcal{B}^P(X) = \{\{\hat{Y} = \pi_0(\hat{Y}|X, \tau) \mid \tau \in \mathcal{T}(X)\}\}. \quad (5)$$

196

3.3 OUTCOME VOLATILITY

198 In addition to procedural volatility, we also consider variations in the final answers. During pol-
 199 icy optimization, diverse answers to a question induce gradients from multiple directions, helping
 200 the model avoid pitfalls from different sources. To quantify this diversity, we introduce outcome
 201 volatility, which evaluates the inconsistencies in the final answers (outcomes) produced by different
 202 possible reasoning trajectories sampled from the policy.

203 In particular, given the original policy (the LLM before RLVR training) π_0 and a question $X \in \mathcal{Q}$
 204 under consideration, we directly sample n_O outputs from the policy to obtain a multiset, *i.e.*,

$$206 \quad \mathcal{B}^O(X) = \{\{\hat{Y}_i \mid i = 1, 2, \dots, n_O, \hat{Y}_i \sim \pi_0(\hat{Y}|X)\}\}. \quad (6)$$

208

3.4 CONFORMAL PREDICTION

209 Procedural volatility and outcome volatility generate multisets for each instance, encompassing the
 210 possible answers of LLMs. We are now concerned with how many of these answers are *likely* to
 211 be the correct answer. To address this, we employ conformal prediction (Vovk et al., 2005; Su
 212 et al., 2024) as a theoretically grounded solution. The overall procedures of computing conformal

214 ¹Different from sets, multisets (bags) allow repetition of elements, with each element associated with a
 215 count of its appearance. For convenience, we use $|\cdot|$ to denote the size of the multiset, defined as the sum of
 the counts of all elements, and \uplus to denote the union of multisets, where the counts of each element are added.

216

217

Algorithm 1: The execution pipeline of CONST

```

18   Input: The set of questions  $Q$ , the original policy  $\pi_0$ , the calibration set  $\mathcal{D}^{\text{cal}} = \{(X_i^{\text{cal}}, Y_i^{\text{cal}})\}_{i=1}^m$ 
19   1 Initialize CalScoreList and SizeList as empty lists
20   2 for iteration  $i \leftarrow 1$  to  $m$  do // Calibrate the scoring function
21   3   | Calculate the score  $f^{\pi_0}(X_i^{\text{cal}}, Y_i^{\text{cal}})$  with Eq. 9 and append it to CalScoreList
22   4 end
23   5 Find the  $\frac{(m+1)(1-\alpha)}{m}$  quantile of CalScoreList as  $\hat{\rho}$ 
24   6 for iteration  $i \leftarrow 1$  to  $N$  do // Obtain the conformal prediction sets
25   7   | Calculate the multiset of possible answers  $\mathcal{B}(X_i)$  according to Eq. 5 and Eq. 6
26   8   | Calculate the score  $f^{\pi_0}(X_i, \hat{Y}_i)$  for each  $\hat{Y}_i \in \mathcal{B}(X_i)$  with Eq. 9
27   9   | Obtain the prediction set  $\hat{\mathcal{C}}_{1-\alpha}(X)$  with  $\hat{\rho}$  using Eq. 10 and append the size of it to SizeList
28 10 end
29 11 Cluster  $Q$  into  $b$  groups  $Q_1, Q_2, \dots, Q_b$ 
30 12 Select the question with the largest size from each group to form  $Q'$  // Select critical samples
31 13 Annotate  $Q'$  with ground truth answers  $\mathcal{A}'$  // Annotate several samples
32 14 Optimize  $\pi_0$  with  $Q'$  and  $\mathcal{A}'$  to obtain the optimized model  $\pi^P$  // Optimize the policy using RL
33 15 return  $\pi^P$  as the optimized model

```

233

234

prediction sets have been discussed in Section 2, and in the following, we will present the design of the scoring function f and how the prediction sets $\mathcal{C}_{1-\alpha}(X)$, $X \in \mathcal{Q}$ are obtained.

As discussed in Section 2, the scoring function $f^{\pi_0}(X, Y) \in \mathbb{R}$ is designed to quantify the disagreement between the input question X and the final answer Y . In other words, when the model $\pi_0(Y|X)$ is certain that Y is the correct answer given the input X , $f^{\pi_0}(X, Y)$ will be low, and vice versa. Conformal prediction does not require the scoring function to have theoretical guarantees of the measurement of certainty, although a good measurement is preferred. For each input question $X \in \mathcal{Q}$ and a predicted answer $\hat{Y} \in \mathcal{B}(X) = \mathcal{B}^P(X) \uplus \mathcal{B}^O(X)$, we compute the scoring function by comparing \hat{Y} with other elements in $\mathcal{B}(X)$. Specifically, as consistent predictions are a natural sign of certainty (Wang et al., 2022), we use the negative frequency of \hat{Y} in $\mathcal{B}(X)$, i.e.,

$$f_{\text{NF}}(X, \widehat{Y}) = -\text{freq}(\widehat{Y}; \mathcal{B}(X)) = -\frac{\text{count}_{\mathcal{B}(X)}(\widehat{Y})}{|\mathcal{B}(X)|}, \quad (7)$$

where $\text{count}_{\mathcal{B}(X)}(\cdot)$ returns the number of elements in the multiset. Nevertheless, using negative frequency alone as the scoring function may cause the scores to be concentrated on certain values, and therefore, entropy is used for fine-grained measurement, defined as follows:

$$f_{\text{ent}}(X, \hat{Y}) = \frac{H(\mathcal{B}(X))}{\log |\mathcal{B}(X)|} = \frac{-\sum_{Y' \in \text{set}(\mathcal{B}(X))} \text{freq}(Y'; \mathcal{B}(X)) \log \text{freq}(Y'; \mathcal{B}(X))}{\log |\mathcal{B}(X)|}, \quad (8)$$

where $\text{set}(\cdot)$ returns the non-repeating elements in the multiset. Finally, the negative frequency and entropic scores are combined to obtain the final scoring function:

$$f^{\pi_0}(X, \widehat{Y}) \equiv f_{\text{NE}}(X, \widehat{Y}) + \lambda \cdot f_{\text{opt}}(X, \widehat{Y}), \quad (9)$$

259 where λ is a hyperparameter balancing the two terms. With the scoring function, we then calibrate it
 260 with a calibration set as described in Section 2 to obtain the threshold $\hat{\rho}$. Note that when computing
 261 the calibration scores, if the correct answer Y_i^{cal} does not appear in the final multiset $\mathcal{B}(X_i^{\text{cal}})$, we set
 262 the score $f(X_i^{\text{cal}}, Y_i^{\text{cal}})$ to $+\infty$. Thus, we obtain the conformal prediction set for each $X \in \mathcal{Q}$ as:

$$\widehat{\mathcal{C}}_{1-\alpha}(X) = \{\widehat{Y} \in \text{set}(\mathcal{B}(X)) \mid f^{\pi_0}(X, \widehat{Y}) < \widehat{\rho}\}. \quad (10)$$

264

3.5 MODEL OPTIMIZATION

268 The size of the conformal prediction set naturally measures how many of the answers that the model
269 considers likely to be correct. A larger size indicates richer and more effective optimization sig-
nals associated with the correct answer during model training. Therefore, we use the size of the

270 conformal prediction set as the criterion for selecting critical samples. Additionally, to encourage
 271 sample diversity, we cluster the set of questions \mathcal{Q} into b groups $\mathcal{Q}_1, \mathcal{Q}_2, \dots, \mathcal{Q}_b$ before selecting
 272 the samples from each group. Formally, the selection process can be written as follows:

$$273 \quad 274 \quad \mathcal{Q}' = \left\{ \arg \max_{X \in \mathcal{Q}_i} |\widehat{\mathcal{C}}_{1-\alpha}(X)| \mid i = 1, 2, \dots, b \right\}. \quad 275$$

276 With the selected set of questions $\mathcal{Q}' \subset \mathcal{Q}$, we annotate this small subset to obtain its ground truth
 277 answers \mathcal{A}' . Finally, we use the standard RLVR algorithm (*i.e.*, GRPO), as described in Section 2, to
 278 optimize the model π_0 with \mathcal{Q}' and \mathcal{A}' to obtain π^P as our final model. A summary of the execution
 279 pipeline of the proposed CONST is presented in Algorithm 1.

280 3.6 THEORETICAL ANALYSIS

282 Here, we aim to provide a theoretical understanding of our proposed CONST under the *lottery sample hypothesis*. Before going into the details, we first review the basic notions of ergodic Markov
 283 decision processes and mixing time (Puterman, 1990).

285 **Definition 3.1.** A Markov decision process $\mathcal{M} \triangleq (\mathcal{S}, \mathcal{A}, P, r, \gamma)$ is ergodic if the induced Markov
 286 chain under **any** stationary policy admits a unique stationary distribution ρ_∞ . Moreover, the under-
 287 lying Markov chain of an ergodic MDP is said to mix in time $t_{mix}(\epsilon)$ if

$$288 \quad 289 \quad t_{mix}(\epsilon) \triangleq \min\{t \geq 0 : \max_{s \in \mathcal{S}} \left(\max_{A \subseteq \mathcal{S}} (|\Pr(Y_t \in A | Y_0 = s) - \rho_\infty(A)|) \right) \leq \epsilon\},$$

290 where $(Y_0, Y_1, \dots, Y_t, \dots)$ denotes an induced Markov chain under any stationary policy and $\epsilon > 0$.

291 **Remark 3.1.** When $\epsilon < 1/2$, choosing a different ϵ only changes the mixing time up to a constant
 292 factor (Levin & Peres, 2017) and so one often fixes $\epsilon = 1/4$ and simply writes $t_{mix} \triangleq t_{mix}(1/4)$.

294 With the concept of ergodic MDP, we next establish a generalization bound for our proposed CONST
 295 under the *lottery sample hypothesis*. Before doing so, we first introduce some frequently used no-
 296 tations. Specifically, since CONST only utilizes a subset of training instances $\mathcal{Q}' \subset \mathcal{Q}$ to optimize
 297 policy π_θ where $|\mathcal{Q}'| = b$. So, for any subset $S \subset \mathcal{Q}$, we define the empirical GRPO loss on S as
 298 follows:

$$299 \quad \hat{\mathcal{L}}_{GRPO}^S = -\frac{1}{n|S|} \sum_{X \in S} \sum_{i=1}^n \min \left(\frac{\pi_\theta(O_i | X)}{\pi_{\theta'}(O_i | X)} a_i, \text{clip} \left(\frac{\pi_\theta(O_i | X)}{\pi_{\theta'}(O_i | X)}, 1 - \varepsilon, 1 + \varepsilon \right) a_i \right) + \mathcal{D}_{KL}(\pi_\theta || \pi_0),$$

301 where $a_i \triangleq \frac{r_i - \text{mean}(\{r_j\}_{j \in S})}{\text{std}(\{r_j\}_{j \in S})}$ is the advantage calculated based on relative rewards. With this
 302 symbol, we then present the approximation assumption about the chosen subset \mathcal{Q}' , that is to say,

304 **Assumption 3.1** (Lottery Sample Hypothesis). *Subset \mathcal{Q}' is said to be an ϵ -approximation of the full
 305 training set $\mathcal{Q} \triangleq \{X_1, X_2, \dots, X_N\}$ if $\|\nabla \hat{\mathcal{L}}_{GRPO}^{\mathcal{Q}'}(\theta) - \nabla \hat{\mathcal{L}}_{GRPO}^{\mathcal{Q}}(\theta)\|_2 \leq \epsilon$ holds for any parameter
 306 vector θ where the symbol $\|\cdot\|_2$ denotes l_2 norm and $\epsilon > 0$.*

307 Next, we make some standard assumptions in optimization theory (Li et al., 2018; Yue et al., 2023).

309 **Assumption 3.2** (Smoothness). *The objective $\hat{\mathcal{L}}_{GRPO}^{\mathcal{Q}}(\theta)$ is L -smooth, that is, $\hat{\mathcal{L}}_{GRPO}^{\mathcal{Q}}(\theta)$ is differen-
 310 tiable and there exists a constant $L > 0$ such that $\|\nabla \hat{\mathcal{L}}_{GRPO}^{\mathcal{Q}}(x) - \nabla \hat{\mathcal{L}}_{GRPO}^{\mathcal{Q}}(y)\|_2 \leq L\|x - y\|_2$.*

311 **Assumption 3.3** (Polyak-Łojasiewicz Condition). *There exists a constant $\mu > 0$ such that
 312 $2\mu(\hat{\mathcal{L}}_{GRPO}^{\mathcal{Q}}(\theta) - \hat{\mathcal{L}}_{GRPO}^{\mathcal{Q}}(\theta_{GRPO}^*)) \leq \|\nabla \hat{\mathcal{L}}_{GRPO}^{\mathcal{Q}}(\theta)\|_2^2$ where $\theta_{GRPO}^* \triangleq \arg \min_{\theta} \hat{\mathcal{L}}_{GRPO}^{\mathcal{Q}}(\theta)$.*

313 Furthermore, we suppose, at line 14 of Algorithm 1, the policy parameter vector θ is updated by stan-
 314 dard gradient descent, *i.e.*, $\theta_{k+1} \triangleq \theta_k - \frac{1}{L} \nabla \hat{\mathcal{L}}_{GRPO}^{\mathcal{Q}'}(\theta)$, where L denotes the smoothness parameter.
 315 With all these preparations, we can have the following generalization theorem:

316 **Theorem 3.1** (Proof is deferred to Appendix A). *Under Assumption 3.1-3.3, if the underlying MDP
 317 $\mathcal{M} \triangleq (\mathcal{S}, \mathcal{A}, P, r, \gamma)$ is ergodic with mixed time t_{mix} and the gradient $\nabla \hat{\mathcal{L}}_{GRPO}^{\mathcal{Q}}(\theta)$ is bounded, *i.e.*,
 318 $\|\nabla \hat{\mathcal{L}}_{GRPO}^{\mathcal{Q}}(\theta)\|_2 \leq G$, then the following inequality holds with probability greater than $1 - \delta$, that is,*

$$320 \quad 321 \quad \mathcal{L}_{GRPO}(\theta_k) - \mathcal{L}_{GRPO}(\theta^*) \leq 4\mathcal{R}(\mathcal{F}_{GR}) + \mathcal{O} \left(\sqrt{\frac{t_{mix}\sigma_R^2(1 - \frac{1}{n})\ln(\frac{1}{\delta})}{Nn}} + \frac{\ln(\frac{1}{\delta})}{Nn(1 - \gamma)} \right) \\ 322 \quad 323 \quad + (1 - \frac{\mu}{L})^{k+1} \hat{\mathcal{L}}_{GRPO}^{\mathcal{Q}}(\theta_0) + \frac{2G}{\mu}\epsilon + \frac{\epsilon^2}{2\mu},$$

324 where $\theta^* \triangleq \arg \min_{\theta} \mathcal{L}_{GRPO}(\theta)$, $\mathcal{R}(\mathcal{F}_{GR})$ is the Rademacher complexity of the group-relative loss
 325 function space \mathcal{F}_{GR} , N denotes the size of full training set \mathcal{Q} , n is size of outputs for each question
 326 and σ_R^2 is an upper bound of variance of the return $\{r_i\}_{i=1}^n$, i.e., $\text{Var}_{\pi_{\theta}}(r_i) \leq \sigma_R^2, \forall \theta$.
 327

Remark 3.2. Note that Rademacher complexity serves as a measure of the policy network’s capacity
 328 to fit the training data, reflecting the richness of the function class it can represent. As a result, under
 329 the Lottery Sample Hypothesis, Theorem 3.1 implies that with sufficiently large question dataset and
 330 verified rewards, our proposed **CONST** can effectively approximate the optimal policy parameter θ^* .
 331

332 4 EXPERIMENTS

334 4.1 EXPERIMENTAL SETUP

336 **Datasets and Evaluation.** During model training, we use the BigMath-sub dataset, a randomly
 337 selected subset containing 2048 instances of the BigMath dataset (Albalak et al., 2025). During the
 338 test phase, we use four mathematical reasoning datasets widely adopted in RLVR evaluation, i.e.,
 339 AMC 23 (problems & solutions, 2023), MinervaMath (Lewkowycz et al., 2022), OlympiadBench
 340 (He et al., 2024), and MATH500 (Hendrycks et al., 2021c; Lightman et al., 2023), with details
 341 deferred to Appendix B.1. In the experiments, we report the avg@256 accuracy metric for the
 342 smaller AMC23 dataset, and avg@32 for other datasets following prior works (Zuo et al., 2025;
 343 Wang et al., 2025c). To reduce randomness in instance selection, we repeat the algorithms three
 344 times and report the average result. More details can be found in Appendix B.2.

345 **Baselines.** We compare the proposed **CONST** against various baselines, i.e., (1) NoFinetuning, which
 346 uses the original model for inference, (2) RandSelect, which annotates randomly selected instances
 347 for training, (3) active learning algorithms, including EntSampling (Settles, 1995), BADGE (Ash
 348 et al., 2020), and CEC (Safaei & Patel, 2025), and (4) reasoning-specific selection strategies, includ-
 349 ing SCF (Wang et al., 2022) and EWS (Beygelzimer et al., 2009). More details about the baseline
 350 methods can be found in Appendix B.3 and Appendix C.3.

351 **Implementation Details.** We adopt LLaMA-3.1-8B-Instruct (Grattafiori et al., 2024),
 352 DeepSeek-R1-Distill-Qwen-1.5B (Guo et al., 2025), Qwen2.5-Math-1.5B, and
 353 Qwen2.5-Math-7B (Yang et al., 2024) for RLVR training. For the calibration set, we use 1024
 354 instances randomly selected from BigMath (ensuring no overlap with BigMath-sub), and to justify
 355 the robustness of **CONST** to the choice of the calibration set, MMLU (Hendrycks et al., 2021a;b)
 356 is used as an alternative. For procedural volatility, we set the number of stages n_P to 20, and for
 357 outcome volatility, we set n_O to 20. In conformal prediction, we set the error rate α to 0.1 and λ
 358 to 0.02. For the budget of annotation, we report the results of 4 and 8 instances. For the clustering
 359 step, we use Sentence-BERT (Reimers & Gurevych, 2019) to obtain the embeddings of the input
 360 queries, and use the K-means algorithm to obtain the clusters. The number of clusters is set to b ,
 361 which is the budget of annotation. For the RLVR optimization hyperparameter setup, we generally
 362 follow the training configuration of Wang et al. (2025c). By default, we set the maximum number
 363 of tokens to 8192 in training and 3072 in inference, the learning rate to 1×10^{-6} , the weight decay
 364 to 0.01, the hyperparameter of β in GRPO (Eq. 2) to 1×10^{-3} , the batch size to 64, and 8 gradient
 365 updates for each rollout. We train the model for at most 500 iterations and evaluate the model every
 366 20 iterations. During training, we duplicate the samples to occupy a single batch. We use the VERL
 367 framework (Sheng et al., 2024) for RLVR training and inference. For the computation hardware, we
 368 use 4 NVIDIA H800 for both training and inference.

369 4.2 PERFORMANCE COMPARISON

370 We compare the proposed **CONST** with various baselines across different LLM architectures on four
 371 mathematical reasoning datasets with varying budget sizes, and report the avg@32 (avg@256)
 372 metric in Table 1. According to the results, we make several observations (Obs.) listed as fol-
 373 lows: **Obs. 1** **CONST significantly improves vanilla models across various scenarios, outper-**
 374 **forming baselines.** For example, using only 8 critical instances, **CONST** significantly improves vanilla
 375 LLaMA-3.1-8B-Instruct by 40.71%, DeepSeek-R1-Distill-Qwen-1.5B by 70.65%,
 376 and Qwen2.5-Math-1.5B by 76.76%, surpassing competitive active learning baselines not de-
 377 signed for reinforcement learning on LLMs (e.g., BADGE and CEC). **Obs. 2** **Training on critical**
 378 **instances discovered by CONST achieves comparable results to training on the full dataset.** The

378
 379 Table 1: Performance comparison with various baselines and training on the full dataset under the
 380 avg@32 (avg@256 for AMC23) metric. We mark the best in **bold** and runner-ups with underline.
 381

Datasets	AMC23		MinervaMath		OlympiadBench		MATH500		AVG	
Budget	4	8	4	8	4	8	4	8	4	8
LLaMA-3.1-8B-Instruct										
NoFinetuning	18.03		14.37		12.28		35.79		20.12	
RandSelect	19.48	18.34	16.77	18.05	<u>13.54</u>	13.87	39.02	39.03	22.20	22.32
EntSampling	<u>20.42</u>	19.70	16.66	18.12	13.43	13.14	37.29	36.33	21.95	21.82
BADGE	19.34	20.02	<u>20.25</u>	<u>19.28</u>	13.27	13.81	<u>41.72</u>	42.68	<u>23.95</u>	23.65
CEC	20.25	<u>21.24</u>	16.66	18.50	13.05	<u>15.02</u>	38.03	<u>42.97</u>	21.79	<u>24.43</u>
CONST (ours)	20.62	24.27	21.68	24.19	16.83	17.61	43.46	47.17	25.65	28.31
FullDataset	24.30		20.99		18.23		48.58		28.03	
DeepSeek-R1-Distill-Qwen-1.5B										
NoFinetuning	30.94		14.17		17.68		50.03		28.21	
RandSelect	40.96	54.55	19.28	<u>23.31</u>	25.02	<u>33.68</u>	64.29	<u>72.96</u>	37.39	<u>46.13</u>
EntSampling	<u>54.91</u>	54.88	22.23	22.55	<u>32.68</u>	32.98	<u>71.79</u>	71.97	<u>45.40</u>	45.60
BADGE	42.84	50.13	21.39	23.20	27.62	30.76	67.73	71.04	39.90	43.78
CEC	49.75	51.46	21.88	22.14	30.50	31.50	69.96	71.44	43.02	44.14
CONST (ours)	55.84	59.16	23.17	23.66	33.66	34.90	73.61	74.84	46.57	48.14
FullDataset	60.27		24.55		36.30		75.49		49.15	
Qwen2.5-Math-1.5B										
NoFinetuning	31.74		9.47		21.72		36.23		24.79	
RandSelect	<u>44.66</u>	<u>46.88</u>	15.19	<u>21.35</u>	<u>30.94</u>	30.46	<u>64.32</u>	65.74	38.78	41.11
EntSampling	40.64	42.43	17.69	20.62	27.24	27.32	59.79	62.26	36.34	38.16
BADGE	44.61	46.73	<u>19.91</u>	20.97	28.87	29.54	63.69	64.88	<u>39.27</u>	40.53
CEC	42.42	45.32	13.67	21.24	28.00	30.88	59.11	<u>68.87</u>	35.80	<u>41.58</u>
CONST (ours)	47.19	48.42	20.01	24.54	32.05	32.75	67.68	69.58	41.73	43.82
FullDataset	49.13		24.30		33.33		70.88		44.41	
Owen2.5-Math-7B										
NoFinetuning	56.04		33.90		37.28		81.03		52.06	
RandSelect	<u>57.05</u>	<u>57.48</u>	<u>35.26</u>	<u>35.91</u>	<u>38.29</u>	<u>38.77</u>	<u>81.58</u>	<u>81.90</u>	<u>53.05</u>	<u>53.52</u>
EntSampling	56.95	<u>57.87</u>	<u>35.36</u>	35.37	<u>38.46</u>	38.63	<u>81.88</u>	81.89	<u>53.16</u>	53.44
BADGE	54.36	56.76	34.12	35.08	<u>37.63</u>	38.92	80.81	<u>82.25</u>	51.73	53.25
CEC	56.03	<u>58.28</u>	34.73	35.21	38.41	<u>39.18</u>	81.70	82.16	52.72	<u>53.71</u>
CONST (ours)	58.21	59.05	35.83	36.97	39.56	40.19	82.94	83.55	54.14	54.94
FullDataset	58.70		36.66		41.04		83.61		55.00	

410 results in Table 1 demonstrate that with less than 0.5% of the samples selected by **CONST** in an *unsupervised manner*, we can achieve very similar performance on average: less than 1.09% difference
 411 in terms of avg@k accuracy for budget 8. This confirms the value of these lottery-winning samples
 412 and our method that discovers them without access to ground truth answers.
 413

415 4.3 ABLATION STUDIES

417 We then investigate how the different components or mechanisms in **CONST** affect the final performance. In particular, we design six variants of **CONST**, denoted as V1
 418 to V6. V1 removes conformal prediction and randomly selects instances from each cluster. V2 skips clustering and chooses samples with the largest conformal prediction sets. V3 uses entropy in Eq. 8 instead of conformal prediction sets to select instances in each cluster. V4 explores alternative configurations in Eq. 11 by clustering instances into $b/2$ groups and selecting the top 2 items with the highest conformal prediction sets. V5 removes procedural volatility, and V6 removes outcome volatility. We perform experiments on LLaMA-3.1-8B-Instruct with the budget of 8, and the results in terms of avg@32 (avg@256) are shown in Table 2, from which we have the following observations: **Obs. 3** **All components or mechanisms in CONST contribute to the final performance.** As shown in the table, removing any of the proposed techniques consistently decreases accuracy across datasets,

419 Table 2: Ablation study of **CONST** with the budget of 8.

Variants	AMC23	Minerva Math	Olympiad Bench	MATH 500	AVG
V1	20.87	16.89	13.76	40.53	23.01
V2	22.03	21.37	15.18	43.60	25.54
V3	19.98	17.64	14.79	40.79	23.30
V4	22.97	25.02	17.11	45.31	27.60
V5	23.96	20.21	16.56	44.80	26.38
V6	21.16	16.34	14.50	40.16	23.04
CONST	24.27	24.19	17.61	47.17	28.31

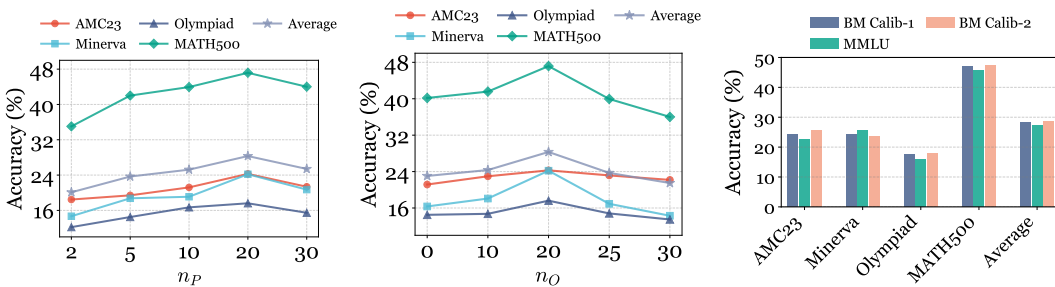


Figure 3: **Left:** performance under different numbers of stages (n_P). **Middle:** performance under different numbers of samples (n_O). **Right:** robustness to different choices of the calibration set.

demonstrating the effectiveness of conformal prediction, procedural/outcome volatility, and clustering. **Obs.④ Conformal prediction plays an important role.** The results show that replacing conformal prediction with alternatives such as random selection or entropy selection leads to severe performance degradation (*i.e.*, 5% drop in terms of absolute accuracy).

4.4 FURTHER ANALYSIS

Performance under Different Hyperparameters. We then show the model’s performance (in terms of $\text{avg}@32/\text{avg}@256$) under different hyperparameters: the number of stages (*i.e.*, n_P) in procedural volatility (Eq. 4) and the number of samples (*i.e.*, n_O) in outcome volatility (Eq. 6). The experimental results on LLaMA-3.1-8B-Instruct are shown in Figure 3 (Left and Middle). From the results, we observe that: **Obs.⑤ Both n_P and n_O achieve best performance at 20.** The number of stages n_P controls the granularity of procedural volatility: when the granularity is too coarse (small n_P s), it may be difficult to capture the twists and turns in the reasoning trajectories; when the granularity is small (large n_P s), it may frequently interrupt the logic fragments. On the other hand, n_O controls the balance of procedural volatility and outcome volatility in the multiset $\mathcal{B}(X)$, which affects the scoring function and thus conformal prediction sets.

Robustness to Different Choice of Calibration Sets. CONST requires a calibration set, and therefore, we also investigate the method’s robustness under different choices of the calibration sets. Specifically, we adopt three sets: (1) *BM Calib-1*, which is the original one; (2) *BM Calib-2*, which is also sampled from the BigMath dataset with no overlap with the training set; (3) *MMLU*, which contains mathematical questions from the MMLU dataset. The results on LLaMA are presented in Figure 3 (Right), and we observe that: **Obs.⑥ The proposed method is robust to the choice of calibration sets.** Using a calibration set with identical distributions to the training set (*i.e.*, *BM Calib-1* and *BM Calib-2*) yields similar high accuracy on average. When using a calibration set with a different distribution (*i.e.*, *MMLU*), there is a slight decrease, but the difference is marginal on average, showing that CONST is robust to the different choices of the calibration set. **The results also indicate that it is possible to use existing datasets that are already annotated (*e.g.*, *MMLU*) as the calibration set to avoid the need to annotate the calibration set.**

4.5 PRELIMINARY RESULTS ON ACTIVE LOOPS

We further explore the potential of CONST in an active loop. Specifically, we use the LLaMA-3.1-8B-Instruct model fine-tuned in the initial round (CONST-1) as the updated policy, and re-evaluated the remaining unlabeled instances in the training set to select a new batch of samples with the same budget of $b = 8$. The model was then further optimized, starting from the checkpoint of the previous round (denoted as CONST-2). The performance comparison are shown in Table 3. As we can see from the results, the iterative selection and optimization using CONST yields consistent performance gains across all datasets, raising the average accuracy from 28.31% to 30.64%. This suggests that: **Obs.⑦ As the policy evolves, CONST can effectively re-identify critical instances, achieving continuous improvement.** The proposed CONST can perform better with more computation and even surpassing the baseline that trains on the full dataset.

Table 3: Performance comparison with the budget of 8 between the initial round (CONST-1) and the subsequent active learning round (CONST-2).

Round	AMC23	Minerva Math	Olympiad Bench	MATH 500	AVG
CONST-1	24.27	24.19	17.61	47.17	28.31
CONST-2	25.29	27.31	18.73	51.24	30.64

486 5 RELATED WORKS

488 **Reinforcement Learning for LLM Reasoning.** Reinforcement learning (Sutton et al., 1999;
 489 Havrilla et al., 2024a; Wen et al., 2024; Liu et al., 2025a) has significantly enhanced the reasoning
 490 capabilities of LLMs via rewards from verifiable answers (Shao et al., 2024; Mroueh, 2025;
 491 Wen et al., 2025) or reward models (Dong et al., 2024; Setlur et al., 2024; Rita et al., 2024; Qu et al.,
 492 2025). Early efforts (Sprueill et al., 2023; Deng et al., 2024; Wang et al., 2024) mainly focus on supervising the LLMs’ reasoning process, often involving the value functions (Havrilla et al., 2024b;
 493 Zhai et al., 2025; Yuan et al., 2025; Zhang et al., 2025a). More recently, outcome supervision,
 494 with the reward obtained from verifiable ground truth answers, has received increasing attention
 495 (Shao et al., 2024; Liu et al., 2025b; Su et al., 2025; Liu et al., 2025c), due to its simplicity and the
 496 immunity from reward hacking (Gao et al., 2024; Fu et al., 2025; Miao et al., 2025).
 497

498 **Conformal Prediction.** Conformal prediction (Vovk et al., 2005; Tibshirani et al., 2019; Angelopoulos et al., 2023; Straitouri et al., 2023; Kiyani et al., 2024a; Gibbs et al., 2025) is a model-
 499 agnostic and distribution-free solution of uncertainty quantification (Stracuzzi et al., 2017; Wang
 500 et al., 2019; Psaros et al., 2023), with solid mathematical foundations (Fontana et al., 2023; An-
 501 gelopoulos et al., 2024). It generates prediction sets that contain the ground truth answer under a
 502 predefined error rate. While most prior efforts focus on conformal prediction with smaller classi-
 503 fication or regression models (Correia et al., 2024; Jeary et al., 2024; Cresswell et al., 2024; Zhou
 504 et al., 2025), its adoption in natural language processing (Campos et al., 2024), and particularly
 505 LLMs (Cherian et al., 2024; Kiyani et al., 2024b; Su et al., 2024; Mohri & Hashimoto, 2024; Wang
 506 et al., 2025b; Chankaev & Ilyushin, 2025), has received increasing attention. Compared to these
 507 prior works, this paper uses conformal prediction to guide the selection of critical samples.
 508

509 **Active Learning.** Active learning (Cohn et al., 1994; 1996; Baram et al., 2004; Castro et al.,
 510 2008; Ren et al., 2021) aims to optimize deep learning models with limited annotation efforts. It is
 511 particularly useful when the ground truth answers can only be obtained with relatively high costs
 512 (Konyushkova et al., 2017; Yuan et al., 2023; Xiao et al., 2023; Chen et al., 2024). With the success
 513 of LLMs, efforts have been made in both LLM for active learning, which uses LLMs for active an-
 514 notation (Margatina et al., 2023; Melo et al., 2024; Li et al., 2024; Kholodna et al., 2024; Ceravolo
 515 et al., 2024; Astorga et al., 2024; Xia et al., 2025), and active learning for LLMs, which adopts active
 516 learning for optimizing LLMs (Muldrew et al., 2024; Sun et al., 2024; Zhang et al., 2024a; Hübotter
 517 et al., 2024; Zhang et al., 2024b). In this paper, we explore active learning to optimize the reasoning
 518 capability of LLMs with a data-efficient and performance-competitive reasoning framework.
 519

520 **Data Selection and Valuation.** Data selection and valuation (Das et al., 2020; Paul et al., 2021;
 521 Killamsetty et al., 2021; Guo et al., 2022; Wang & Jia, 2023; Das et al., 2024; Ebiele et al., 2025)
 522 aim to find the most valuable data in the training set to save computational resources. For example,
 523 Paul et al. (Paul et al., 2021) use the loss function and its gradients to select important examples
 524 very early in training. Guo et al. (Guo et al., 2022) provide a comprehensive code library in addition
 525 to extensive evaluation for data subset selection and valuation. Das et al. (Das et al., 2024) propose
 526 CheckSelect, a flexible, accurate, robust, and efficient method for extracting the high-value subsets.
 527 Nevertheless, many works on data subset selection and valuation assume complete annotation of the
 528 training set by computing the loss function or its gradients (Paul et al., 2021; Wang & Jia, 2023;
 529 Das et al., 2024), and conducted primarily in the domain of vision (Das et al., 2020; 2021a; Paul
 530 et al., 2021). By comparison, this work proposes **CONST** that aims to find important training data
 531 (the critical instances) without the annotation, and only annotate the important instances to achieve
 532 annotation-efficient RLVR optimization of LLMs.
 533

6 CONCLUSION

534 This paper investigates an important question: how can we identify the lottery-winning samples
 535 from the original dataset without access to answers, thereby enabling an annotation-minimal, data-
 536 efficient and performance-competitive alternative for optimizing the reasoning capability of LLMs.
 537 Through the design of our novel **CONST** framework, a probabilistic method grounded in the mathe-
 538 matical foundation of conformal prediction and incorporating complementary considerations of pro-
 539 cedural and outcome volatility, we demonstrate that the unsupervised discovery of critical instances
 in full datasets can achieve comparable performance with significantly less annotation efforts.
 540

540 REFERENCES
541

542 Alon Albalak, Duy Phung, Nathan Lile, Rafael Rafailov, Kanishk Gandhi, Louis Castricato, Anikait
543 Singh, Chase Blagden, Violet Xiang, Dakota Mahan, and Nick Haber. Big-math: A large-scale,
544 high-quality math dataset for reinforcement learning in language models, 2025.

545 Anastasios N Angelopoulos, Stephen Bates, et al. Conformal prediction: A gentle introduction.
546 *Foundations and trends in machine learning*, 16(4):494–591, 2023.

547 Anastasios N Angelopoulos, Rina Foygel Barber, and Stephen Bates. Theoretical foundations of
548 conformal prediction. *arXiv preprint arXiv:2411.11824*, 2024.

549 Rohan Anil, Sebastian Borgeaud, Jean-Baptiste Alayrac, Jiahui Yu, Radu Soricut, Johan Schalkwyk,
550 Andrew M Dai, Anja Hauth, Katie Millican, et al. Gemini: a family of highly capable multimodal
551 models. *arXiv preprint arXiv:2312.11805*, 2023.

552 Jordan T Ash, Chicheng Zhang, Akshay Krishnamurthy, John Langford, and Alekh Agarwal. Deep
553 batch active learning by diverse, uncertain gradient lower bounds. In *International Conference on
554 Learning Representations*, 2020.

555 Nicolás Astorga, Tennison Liu, Nabeel Seedat, and Mihaela van der Schaar. Active learning with
556 llms for partially observed and cost-aware scenarios. *Advances in Neural Information Processing
557 Systems*, 37:20819–20857, 2024.

558 Yoram Baram, Ran El Yaniv, and Kobi Luz. Online choice of active learning algorithms. *Journal of
559 Machine Learning Research*, 5(Mar):255–291, 2004.

560 Rina Foygel Barber, Emmanuel J Candes, Aaditya Ramdas, and Ryan J Tibshirani. Conformal
561 prediction beyond exchangeability. *The Annals of Statistics*, 51(2):816–845, 2023.

562 Alina Beygelzimer, Sanjoy Dasgupta, and John Langford. Importance weighted active learning. In
563 *Proceedings of the 26th annual international conference on machine learning*, pp. 49–56, 2009.

564 Margarida Campos, António Farinhas, Chrysoula Zerva, Mário AT Figueiredo, and André FT Martins.
565 Conformal prediction for natural language processing: A survey. *Transactions of the Association
566 for Computational Linguistics*, 12:1497–1516, 2024.

567 Rui Castro, Charles Kalish, Robert Nowak, Ruichen Qian, Tim Rogers, and Jerry Zhu. Human
568 active learning. *Advances in neural information processing systems*, 21, 2008.

569 Paolo Ceravolo, Fatemeh Mohammadi, and Marta Annamaria Tamborini. Active learning methodology in
570 llms fine-tuning. In *2024 IEEE International Conference on Cyber Security and Resilience
571 (CSR)*, pp. 743–749. IEEE, 2024.

572 Shamil Chankaev and Eugene Ilyushin. Calibration of large language models based on the conformal
573 prediction. *International Journal of Open Information Technologies*, 13(6):10–15, 2025.

574 Jiayi Chen, Benteng Ma, Hengfei Cui, and Yong Xia. Think twice before selection: Federated
575 evidential active learning for medical image analysis with domain shifts. In *Proceedings of the
576 IEEE/CVF Conference on Computer Vision and Pattern Recognition*, pp. 11439–11449, 2024.

577 Minghan Chen, Guikun Chen, Wenguan Wang, and Yi Yang. Seed-grpo: Semantic entropy enhanced
578 grp for uncertainty-aware policy optimization. *arXiv preprint arXiv:2505.12346*, 2025.

579 John Cherian, Isaac Gibbs, and Emmanuel Candes. Large language model validity via enhanced
580 conformal prediction methods. *Advances in Neural Information Processing Systems*, 37:114812–
581 114842, 2024.

582 David Cohn, Les Atlas, and Richard Ladner. Improving generalization with active learning. *Machine
583 learning*, 15(2):201–221, 1994.

584 David A Cohn, Zoubin Ghahramani, and Michael I Jordan. Active learning with statistical models.
585 *Journal of artificial intelligence research*, 4:129–145, 1996.

594 Alvaro Correia, Fabio Valerio Massoli, Christos Louizos, and Arash Behboodi. An information the-
 595oretic perspective on conformal prediction. *Advances in Neural Information Processing Systems*,
 596 37:101000–101041, 2024.

597

598 Jesse C Cresswell, Yi Sui, Bhargava Kumar, and Noël Vouitsis. Conformal prediction sets improve
 599 human decision making. In *International Conference on Machine Learning*, pp. 9439–9457.
 600 PMLR, 2024.

601 Soumi Das, Sayan Mandal, Ashwin Bhoyer, Madhumita Bharde, Niloy Ganguly, Suparna Bhat-
 602 tacharya, and Sourangshu Bhattacharya. Multi-criteria online frame-subset selection for au-
 603 tonomous vehicle videos. *Pattern Recognition Letters*, 133:349–355, 2020.

604

605 Soumi Das, Harikrishna Patibandla, Suparna Bhattacharya, Kshounis Bera, Niloy Ganguly, and
 606 Sourangshu Bhattacharya. Tmcoss: Thresholded multi-criteria online subset selection for data-
 607 efficient autonomous driving. In *Proceedings of the IEEE/CVF International Conference on Com-
 608 puter Vision*, pp. 6341–6350, 2021a.

609 Soumi Das, Arshdeep Singh, Saptarshi Chatterjee, Suparna Bhattacharya, and Sourangshu Bhat-
 610 tacharya. Finding high-value training data subset through differentiable convex programming. In
 611 *Joint European Conference on Machine Learning and Knowledge Discovery in Databases*, pp.
 612 666–681. Springer, 2021b.

613

614 Soumi Das, Manasvi Sagarkar, Suparna Bhattacharya, and Sourangshu Bhattacharya. Checkselect:
 615 Online checkpoint selection for flexible, accurate, robust, and efficient data valuation. *IEEE
 616 Transactions on Artificial Intelligence*, 2024.

617 DeepMind. Ai achieves silver-medal standard solving international mathemati-
 618 cal olympiad problems. [https://deepmind.google/discover/blog/
 619 ai-solves-imo-problems-at-silver-medal-level/](https://deepmind.google/discover/blog/ai-solves-imo-problems-at-silver-medal-level/), 2024.

620

621 Zhirui Deng, Zhicheng Dou, Yutao Zhu, Ji-Rong Wen, Ruibin Xiong, Mang Wang, and Weipeng
 622 Chen. From novice to expert: Llm agent policy optimization via step-wise reinforcement learning.
 623 *arXiv preprint arXiv:2411.03817*, 2024.

624

625 Xinhan Di et al. Enhancing math reasoning in small-sized llms via preview difficulty-aware inter-
 626 vention. *arXiv preprint arXiv:2508.01604*, 2025.

627

628 Hanze Dong, Wei Xiong, Bo Pang, Haoxiang Wang, Han Zhao, Yingbo Zhou, Nan Jiang, Doyen
 629 Sahoo, Caiming Xiong, and Tong Zhang. Rlhf workflow: From reward modeling to online rlhf.
 630 *arXiv preprint arXiv:2405.07863*, 2024.

631

632 Angang Du, Bofei Gao, Bowei Xing, Changjiu Jiang, Cheng Chen, Cheng Li, Chenjun Xiao, Chen-
 633 zhuang Du, Chonghua Liao, et al. Kimi k1. 5: Scaling reinforcement learning with llms. *arXiv
 634 preprint arXiv:2501.12599*, 2025.

635

636 Malick Ebiele, Malika Bendechache, and Rob Brennan. Quantitative data valuation methods: A
 637 systematic review and taxonomy. *ACM Journal of Data and Information Quality*, 17(2):1–39,
 2025.

638

639 Xiequan Fan and Qi-Man Shao. Self-normalized cramér type moderate deviations for martingales
 640 and applications. *Bernoulli*, 31(1):130–161, 2025.

641

642 Matteo Fontana, Gianluca Zeni, and Simone Vantini. Conformal prediction: a unified review of
 643 theory and new challenges. *Bernoulli*, 29(1):1–23, 2023.

644

645 Jiayi Fu, Xuandong Zhao, Chengyuan Yao, Heng Wang, Qi Han, and Yanghua Xiao. Reward shap-
 646 ing to mitigate reward hacking in rlhf. *arXiv preprint arXiv:2502.18770*, 2025.

647

648 Jiaxuan Gao, Shusheng Xu, Wenjie Ye, Weilin Liu, Chuyi He, Wei Fu, Zhiyu Mei, Guangju Wang,
 649 and Yi Wu. On designing effective rl reward at training time for llm reasoning. *arXiv preprint
 650 arXiv:2410.15115*, 2024.

648 Isaac Gibbs, John J Cherian, and Emmanuel J Candès. Conformal prediction with conditional guar-
 649 antees. *Journal of the Royal Statistical Society Series B: Statistical Methodology*, pp. qkaf008,
 650 2025.

651

652 Alessandro Grattafiori et al. The Llama 3 herd of models. *arXiv preprint arXiv:2407.21783*, 2024.
 653 includes LLaMA-3.1-8B-Instruct among other LLaMA 3.1 variants.

654 Chengcheng Guo, Bo Zhao, and Yanbing Bai. Deepcore: A comprehensive library for coreset selec-
 655 tion in deep learning. In *International Conference on Database and Expert Systems Applications*,
 656 pp. 181–195. Springer, 2022.

657

658 Daya Guo, Dejian Yang, Haowei Zhang, Junxiao Song, Ruoyu Zhang, Runxin Xu, Qihao Zhu,
 659 Shirong Ma, Peiyi Wang, Xiao Bi, et al. Deepseek-r1: Incentivizing reasoning capability in llms
 660 via reinforcement learning. *arXiv preprint arXiv:2501.12948*, 2025.

661

662 Yifan Hao, Fangning Chao, Yaqian Hao, Zhaojun Cui, Huan Bai, Haiyu Zhang, Yankai Liu, Chao
 663 Deng, and Junlan Feng. Jt-math: A multi-stage framework for advanced mathematical reasoning
 664 in large language models. *arXiv preprint arXiv:2507.19748*, 2025.

665

666 Alex Havrilla, Yuqing Du, Sharath Chandra Raparthy, Christoforus Nalmpantis, Jane Dwivedi-Yu,
 667 Maksym Zhuravinskyi, Eric Hambro, Sainbayar Sukhaatar, and Roberta Raileanu. Teaching
 668 large language models to reason with reinforcement learning. *arXiv preprint arXiv:2403.04642*,
 2024a.

669

670 Alex Havrilla, Sharath Raparthy, Christoforus Nalmpantis, Jane Dwivedi-Yu, Maksym Zhuravinskyi,
 671 Eric Hambro, and Roberta Raileanu. Glore: When, where, and how to improve llm reasoning
 672 via global and local refinements. *arXiv preprint arXiv:2402.10963*, 2024b.

673

674 Chaoqun He, Renjie Luo, Yuzhuo Bai, Shengding Hu, Zhen Leng Thai, Junhao Shen, Jinyi
 675 Hu, Xu Han, Yujie Huang, Yuxiang Zhang, Jie Liu, Lei Qi, Zhiyuan Liu, and Maosong Sun.
 676 Olympiadbench: A challenging benchmark for promoting agi with olympiad-level bilingual mul-
 677 timodal scientific problems. *arXiv preprint arXiv:2402.14008*, 2024.

678

679 Dan Hendrycks, Collin Burns, Steven Basart, Andrew Critch, Jerry Li, Dawn Song, and Jacob
 680 Steinhardt. Aligning ai with shared human values. *Proceedings of the International Conference
 681 on Learning Representations (ICLR)*, 2021a.

682

683 Dan Hendrycks, Collin Burns, Steven Basart, Andy Zou, Mantas Mazeika, Dawn Song, and Jacob
 684 Steinhardt. Measuring massive multitask language understanding. *Proceedings of the Interna-
 685 tional Conference on Learning Representations (ICLR)*, 2021b.

686

687 Dan Hendrycks, Collin Burns, Saurav Kadavath, Akul Arora, Steven Basart, Eric Tang, Dawn Song,
 688 and Jacob Steinhardt. Measuring mathematical problem solving with the math dataset. *arXiv
 689 preprint arXiv:2103.03874*, 2021c.

690

691 Jonas Hübotter, Sascha Bongni, Ido Hakimi, and Andreas Krause. Efficiently learning at test-time:
 692 Active fine-tuning of llms. *arXiv preprint arXiv:2410.08020*, 2024.

693

694 Linus Jeary, Tom Kuipers, Mehran Hosseini, and Nicola Paoletti. Verifiably robust conformal pre-
 695 diction. *Advances in Neural Information Processing Systems*, 37:4295–4314, 2024.

696

697 Natalia Kholodna, Sahib Julka, Mohammad Khodadadi, Mohammed Nurullah Gumus, and Michael
 698 Granitzer. Llms in the loop: Leveraging large language model annotations for active learning in
 699 low-resource languages. In *Joint European Conference on Machine Learning and Knowledge
 700 Discovery in Databases*, pp. 397–412. Springer, 2024.

701 Krishnateja Killamsetty, Durga Sivasubramanian, Ganesh Ramakrishnan, and Rishabh Iyer. Glister:
 702 Generalization based data subset selection for efficient and robust learning. In *Proceedings of the
 703 AAAI conference on artificial intelligence*, volume 35, pp. 8110–8118, 2021.

704

705 Shayan Kiyani, George J Pappas, and Hamed Hassani. Conformal prediction with learned features.
 706 In *International Conference on Machine Learning*, pp. 24749–24769. PMLR, 2024a.

702 Shayan Kiyani, George J Pappas, and Hamed Hassani. Length optimization in conformal prediction.
 703 *Advances in Neural Information Processing Systems*, 37:99519–99563, 2024b.
 704

705 Ksenia Konyushkova, Raphael Sznitman, and Pascal Fua. Learning active learning from data. *Ad-*
 706 *vances in neural information processing systems*, 30, 2017.

707 Nathan Lambert, Jacob Morrison, Valentina Pyatkin, Shengyi Huang, Hamish Ivison, Faeze Brah-
 708 man, Lester James V Miranda, Alisa Liu, Nouha Dziri, Shane Lyu, et al. Tulu 3: Pushing frontiers
 709 in open language model post-training. *arXiv preprint arXiv:2411.15124*, 2024.

710

711 Guanghui Lan. *First-order and stochastic optimization methods for machine learning*, volume 1.
 712 Springer, 2020.

713

714 David A Levin and Yuval Peres. *Markov chains and mixing times*, volume 107. American Mathe-
 715 matical Soc., 2017.

716

717 Aitor Lewkowycz, Anders Andreassen, David Dohan, Ethan Dyer, Henryk Michalewski, Vinay Ra-
 718 masesh, Ambrose Sloane, Cem Anil, Imanol Schlag, Theo Gutman-Solo, et al. Solving quantitative
 719 reasoning problems with language models. *Advances in neural information processing systems*,
 35:3843–3857, 2022.

720

721 Dongyuan Li, Ying Zhang, Zhen Wang, Shiyin Tan, Satoshi Kosugi, and Manabu Okumura. Ac-
 722 tive learning for abstractive text summarization via llm-determined curriculum and certainty gain
 723 maximization. In *Findings of the Association for Computational Linguistics: EMNLP 2024*, pp.
 8959–8971, 2024.

724

725 Yuanzhi Li, Tengyu Ma, and Hongyang Zhang. Algorithmic regularization in over-parameterized
 726 matrix sensing and neural networks with quadratic activations. In *Conference On Learning The-*
 727 *ory*, pp. 2–47. PMLR, 2018.

728

729 Hunter Lightman, Vineet Kosaraju, Yuri Burda, Harrison Edwards, Bowen Baker, Teddy Lee, Jan
 730 Leike, John Schulman, Ilya Sutskever, and Karl Cobbe. Let’s verify step by step. In *The Twelfth
 International Conference on Learning Representations*, 2023.

731

732 Xiaoqian Liu, Ke Wang, Yongbin Li, Yuchuan Wu, Wentao Ma, Aobo Kong, Fei Huang, Jianbin
 733 Jiao, and Junge Zhang. Epo: Explicit policy optimization for strategic reasoning in llms via
 reinforcement learning. *arXiv preprint arXiv:2502.12486*, 2025a.

734

735 Xiaoyuan Liu, Tian Liang, Zhiwei He, Jiahao Xu, Wenxuan Wang, Pinjia He, Zhaopeng Tu, Haitao
 736 Mi, and Dong Yu. Trust, but verify: A self-verification approach to reinforcement learning with
 737 verifiable rewards. *arXiv preprint arXiv:2505.13445*, 2025b.

738

739 Zichen Liu, Changyu Chen, Wenjun Li, Penghui Qi, Tianyu Pang, Chao Du, Wee Sun Lee,
 740 and Min Lin. Understanding r1-zero-like training: A critical perspective. *arXiv preprint
 arXiv:2503.20783*, 2025c.

741

742 Ziru Liu, Cheng Gong, Xinyu Fu, Yaofang Liu, Ran Chen, Shoubo Hu, Suiyun Zhang, Rui Liu,
 743 Qingfu Zhang, and Dandan Tu. Ghpo: Adaptive guidance for stable and efficient llm reinforce-
 744 ment learning. *arXiv preprint arXiv:2507.10628*, 2025d.

745

746 Katerina Margatina, Timo Schick, Nikolaos Aletras, and Jane Dwivedi-Yu. Active learning prin-
 747 ciples for in-context learning with large language models. In *Findings of the Association for
 Computational Linguistics: EMNLP 2023*, pp. 5011–5034, 2023.

748

749 Luckeciano C Melo, Panagiotis Tigas, Alessandro Abate, and Yarin Gal. Deep bayesian active
 750 learning for preference modeling in large language models. *Advances in Neural Information
 Processing Systems*, 37:118052–118085, 2024.

751

752 Yuchun Miao, Sen Zhang, Liang Ding, Yuqi Zhang, Lefei Zhang, and Dacheng Tao. The en-
 753 ergy loss phenomenon in rlhf: A new perspective on mitigating reward hacking. *arXiv preprint
 arXiv:2501.19358*, 2025.

754

755 Michael Mitzenmacher and Eli Upfal. *Probability and computing: Randomization and probabilistic
 techniques in algorithms and data analysis*. Cambridge university press, 2017.

756 Christopher Mohri and Tatsunori Hashimoto. Language models with conformal factuality guar-
 757 antees. In *Proceedings of the 41st International Conference on Machine Learning*, pp. 36029–
 758 36047, 2024.

759

760 Youssef Mroueh. Reinforcement learning with verifiable rewards: Grpo’s effective loss, dynamics,
 761 and success amplification. *arXiv preprint arXiv:2503.06639*, 2025.

762 William Muldrew, Peter Hayes, Mingtian Zhang, and David Barber. Active preference learning for
 763 large language models. *arXiv preprint arXiv:2402.08114*, 2024.

764

765 OpenAI. Learning to reason with llms. <https://openai.com/index/learning-to-reason-with-llms/>, 2024.

766

767 OpenAI. Introducing openai o3 and o4-mini. <https://openai.com/index/introducing-o3-and-o4-mini/>, 2025.

768

769

770 Lei Pang and Ruinan Jin. On the theory and practice of grpo: A trajectory-corrected approach with
 771 fast convergence. *arXiv preprint arXiv:2508.02833*, 2025.

772

773 Harris Papadopoulos, Volodya Vovk, and Alex Gammerman. Conformal prediction with neural
 774 networks. In *19th IEEE International Conference on Tools with Artificial Intelligence (ICTAI*
 775 2007), volume 2, pp. 388–395. IEEE, 2007.

776

777 Mansheej Paul, Surya Ganguli, and Gintare Karolina Dziugaite. Deep learning on a data diet:
 778 Finding important examples early in training. *Advances in neural information processing systems*,
 779 34:20596–20607, 2021.

780

781 Amc problems and solutions. Art of problem solving. https://artofproblemsolving.com/wiki/index.php?title=AMC_Problems_and_Solutions, 2023.

782

783 Apostolos F Psaros, Xuhui Meng, Zongren Zou, Ling Guo, and George Em Karniadakis. Uncer-
 784 tainty quantification in scientific machine learning: Methods, metrics, and comparisons. *Journal*
 785 *of Computational Physics*, 477:111902, 2023.

786

787 Martin L Puterman. Markov decision processes. *Handbooks in operations research and management*
 788 *science*, 2:331–434, 1990.

789

790 Yun Qu, Yuhang Jiang, Boyuan Wang, Yixiu Mao, Cheems Wang, Chang Liu, and Xiangyang
 791 Ji. Latent reward: Llm-empowered credit assignment in episodic reinforcement learning. In
 792 *Proceedings of the AAAI Conference on Artificial Intelligence*, volume 39, pp. 20095–20103,
 793 2025.

794

795 Nils Reimers and Iryna Gurevych. Sentence-bert: Sentence embeddings using siamese bert-
 796 networks. *arXiv preprint arXiv:1908.10084*, 2019.

797

798 Pengzhen Ren, Yun Xiao, Xiaojun Chang, Po-Yao Huang, Zhihui Li, Brij B Gupta, Xiaojiang Chen,
 799 and Xin Wang. A survey of deep active learning. *ACM computing surveys (CSUR)*, 54(9):1–40,
 800 2021.

801

802 ZZ Ren, Zhihong Shao, Junxiao Song, Huajian Xin, Haocheng Wang, Wanjia Zhao, Liyue Zhang,
 803 Zhe Fu, Qihao Zhu, Dejian Yang, et al. Deepseek-prover-v2: Advancing formal mathematical rea-
 804 soning via reinforcement learning for subgoal decomposition. *arXiv preprint arXiv:2504.21801*,
 805 2025.

806

807 Mathieu Rita, Florian Strub, Rahma Chaabouni, Paul Michel, Emmanuel Dupoux, and Olivier
 808 Pietquin. Countering reward over-optimization in llm with demonstration-guided reinforcement
 809 learning. *arXiv preprint arXiv:2404.19409*, 2024.

810

811 Bardia Safaei and Vishal M Patel. Active learning for vision-language models. In *2025 IEEE/CVF*
 812 *Winter Conference on Applications of Computer Vision (WACV)*, pp. 4902–4912. IEEE, 2025.

813

814 John Schulman, Filip Wolski, Prafulla Dhariwal, Alec Radford, and Oleg Klimov. Proximal policy
 815 optimization algorithms. *arXiv preprint arXiv:1707.06347*, 2017.

810 Amrit Setlur, Chirag Nagpal, Adam Fisch, Xinyang Geng, Jacob Eisenstein, Rishabh Agarwal,
 811 Alekh Agarwal, Jonathan Berant, and Aviral Kumar. Rewarding progress: Scaling automated
 812 process verifiers for llm reasoning. *arXiv preprint arXiv:2410.08146*, 2024.

813

814 Burr Settles. Active learning literature survey. *Science*, 10(3):237–304, 1995.

815

816 Shai Shalev-Shwartz and Shai Ben-David. *Understanding machine learning: From theory to algo-*
 817 *rithms*. Cambridge university press, 2014.

818

819 Zhihong Shao, Peiyi Wang, Qihao Zhu, Runxin Xu, Junxiao Song, Xiao Bi, Haowei Zhang,
 820 Mingchuan Zhang, YK Li, Yang Wu, et al. Deepseekmath: Pushing the limits of mathemati-
 821 cal reasoning in open language models. *arXiv preprint arXiv:2402.03300*, 2024.

822

823 Guangming Sheng, Chi Zhang, Zilingfeng Ye, Xibin Wu, Wang Zhang, Ru Zhang, Yanghua Peng,
 824 Haibin Lin, and Chuan Wu. Hybridflow: A flexible and efficient rlhf framework. *arXiv preprint*
 825 *arXiv: 2409.19256*, 2024.

826

827 Henry W Sprueill, Carl Edwards, Mariefel V Olarte, Udishnu Sanyal, Heng Ji, and Sutanay Choud-
 828 hury. Monte carlo thought search: Large language model querying for complex scientific reason-
 829 ing in catalyst design. *arXiv preprint arXiv:2310.14420*, 2023.

830

831 David John Stracuzzi, Maximillian Gene Chen, Michael Christopher Darling, Matthew Gregor Pe-
 832 terson, and Charlie Vollmer. Uncertainty quantification for machine learning. Technical report,
 833 Sandia National Lab.(SNL-NM), Albuquerque, NM (United States), 2017.

834

835 Eleni Straitouri, Lequn Wang, Nastaran Okati, and Manuel Gomez Rodriguez. Improving expert
 836 predictions with conformal prediction. In *International Conference on Machine Learning*, pp.
 837 32633–32653. PMLR, 2023.

838

839 Jiayuan Su, Jing Luo, Hongwei Wang, and Lu Cheng. Api is enough: Conformal prediction for
 840 large language models without logit-access. *arXiv preprint arXiv:2403.01216*, 2024.

841

842 Yi Su, Dian Yu, Linfeng Song, Juntao Li, Haitao Mi, Zhaopeng Tu, Min Zhang, and Dong Yu.
 843 Crossing the reward bridge: Expanding rl with verifiable rewards across diverse domains. *arXiv*
 844 *preprint arXiv:2503.23829*, 2025.

845

846 Zhouhao Sun, LI DU, Xiao Ding, Yixuan Ma, Yang Zhao, Kaitao Qiu, Ting Liu, and Bing Qin.
 847 Causal-guided active learning for debiasing large language models. In *Annual Meeting of the*
 848 *Association for Computational Linguistics*, 2024.

849

850 Richard S Sutton, Andrew G Barto, et al. Reinforcement learning. *Journal of Cognitive Neuro-
 851 science*, 11(1):126–134, 1999.

852

853 Ryan J Tibshirani, Rina Foygel Barber, Emmanuel Candes, and Aaditya Ramdas. Conformal pre-
 854 diction under covariate shift. *Advances in neural information processing systems*, 32, 2019.

855

856 Ilya O Tolstikhin and Yevgeny Seldin. Pac-bayes-empirical-bernstein inequality. *Advances in Neural*
 857 *Information Processing Systems*, 26, 2013.

858

859 Abdullah Vanlioglu. Entropy-guided sequence weighting for efficient exploration in rl-based llm
 860 fine-tuning. *arXiv preprint arXiv:2503.22456*, 2025.

861

862 Vladimir Vovk, Alexander Gammerman, and Glenn Shafer. *Algorithmic learning in a random world*.
 863 Springer, 2005.

864

865 Bin Wang, Jie Lu, Zheng Yan, Huaishao Luo, Tianrui Li, Yu Zheng, and Guangquan Zhang. Deep
 866 uncertainty quantification: A machine learning approach for weather forecasting. In *Proceedings*
 867 *of the 25th ACM SIGKDD international conference on knowledge discovery & data mining*, pp.
 868 2087–2095, 2019.

869

870 Haiming Wang, Mert Unsal, Xiaohan Lin, Mantas Baksys, Junqi Liu, Marco Dos Santos, Flood
 871 Sung, Marina Vinyes, Zhenzhe Ying, Zekai Zhu, et al. Kimina-prover preview: Towards large
 872 formal reasoning models with reinforcement learning. *arXiv preprint arXiv:2504.11354*, 2025a.

864 Huaijie Wang, Shibo Hao, Hanze Dong, Shenao Zhang, Yilin Bao, Ziran Yang, and Yi Wu. Offline
 865 reinforcement learning for llm multi-step reasoning. *arXiv preprint arXiv:2412.16145*, 2024.

866

867 Jiachen T Wang and Ruoxi Jia. Data banzhaf: A robust data valuation framework for machine
 868 learning. In *International Conference on Artificial Intelligence and Statistics*, pp. 6388–6421.
 869 PMLR, 2023.

870 Sean Wang, Yicheng Jiang, Yuxin Tang, Lu Cheng, and Hanjie Chen. Copu: Conformal prediction
 871 for uncertainty quantification in natural language generation. *arXiv preprint arXiv:2502.12601*,
 872 2025b.

873 Xuezhi Wang, Jason Wei, Dale Schuurmans, Quoc Le, Ed Chi, Sharan Narang, Aakanksha Chowdh-
 874 ery, and Denny Zhou. Self-consistency improves chain of thought reasoning in language models.
 875 *arXiv preprint arXiv:2203.11171*, 2022.

876

877 Yiping Wang, Qing Yang, Zhiyuan Zeng, Liliang Ren, Liyuan Liu, Baolin Peng, Hao Cheng, Xuehai
 878 He, Kuan Wang, Jianfeng Gao, et al. Reinforcement learning for reasoning in large language
 879 models with one training example. *arXiv preprint arXiv:2504.20571*, 2025c.

880 Muning Wen, Ziyu Wan, Jun Wang, Weinan Zhang, and Ying Wen. Reinforcing llm agents via policy
 881 optimization with action decomposition. *Advances in Neural Information Processing Systems*, 37:
 882 103774–103805, 2024.

883

884 Xumeng Wen, Zihan Liu, Shun Zheng, Zhijian Xu, Shengyu Ye, Zhirong Wu, Xiao Liang, Yang
 885 Wang, Junjie Li, Ziming Miao, et al. Reinforcement learning with verifiable rewards implicitly
 886 incentivizes correct reasoning in base llms. *arXiv preprint arXiv:2506.14245*, 2025.

887 Lixin Wu, Na Cai, Qiao Cheng, Jiachen Wang, and Yitao Duan. Confucius3-math: A
 888 lightweight high-performance reasoning llm for chinese k-12 mathematics learning. *arXiv
 889 preprint arXiv:2506.18330*, 2025.

890

891 Yu Xia, Subhojoyoti Mukherjee, Zhouhang Xie, Junda Wu, Xintong Li, Ryan Aponte, Hanjia Lyu,
 892 Joe Barrow, Hongjie Chen, Franck Dernoncourt, et al. From selection to generation: A survey of
 893 llm-based active learning. *arXiv preprint arXiv:2502.11767*, 2025.

894

895 Ruixuan Xiao, Yiwen Dong, Junbo Zhao, Runze Wu, Minmin Lin, Gang Chen, and Haobo Wang.
 896 Freeal: Towards human-free active learning in the era of large language models. In *Proceedings of
 897 the 2023 Conference on Empirical Methods in Natural Language Processing*, pp. 14520–14535,
 898 2023.

899

900 An Yang, Beichen Zhang, Binyuan Hui, Bofei Gao, Bowen Yu, Chengpeng Li, Dayiheng Liu,
 901 Jianhong Tu, Jingren Zhou, Junyang Lin, Keming Lu, Mingfeng Xue, Runji Lin, Tianyu Liu,
 902 Xingzhang Ren, and Zhenru Zhang. Qwen2.5-math technical report: Toward mathematical ex-
 903 pert model via self-improvement. *arXiv preprint arXiv:2409.12122*, 2024.

904

905 Di Yuan, Xiaojun Chang, Qiao Liu, Yi Yang, Dehua Wang, Minglei Shu, Zhenyu He, and Guang-
 906 ming Shi. Active learning for deep visual tracking. *IEEE Transactions on Neural Networks and
 907 Learning Systems*, 35(10):13284–13296, 2023.

908

909 Yurun Yuan, Fan Chen, Zeyu Jia, Alexander Rakhlin, and Tengyang Xie. Trajectory bellman residual
 910 minimization: A simple value-based method for llm reasoning. *arXiv preprint arXiv:2505.15311*,
 911 2025.

912

913 Pengyun Yue, Cong Fang, and Zhouchen Lin. On the lower bound of minimizing polyak-łojasiewicz
 914 functions. In *The Thirty Sixth Annual Conference on Learning Theory*, pp. 2948–2968. PMLR,
 915 2023.

916

917 Yuanzhao Zhai, Tingkai Yang, Kele Xu, Dawei Feng, Cheng Yang, Bo Ding, and Huaimin Wang.
 918 Enhancing decision-making for llm agents via step-level q-value models. In *Proceedings of the
 919 AAAI Conference on Artificial Intelligence*, volume 39, pp. 27161–27169, 2025.

920

921 Hongbo Zhang, Han Cui, Guangsheng Bao, Linyi Yang, Jun Wang, and Yue Zhang. Direct value
 922 optimization: Improving chain-of-thought reasoning in llms with refined values. *arXiv preprint
 923 arXiv:2502.13723*, 2025a.

918 Linhai Zhang, Jialong Wu, Deyu Zhou, and Guoqiang Xu. Star: Constraint lora with dynamic
919 active learning for data-efficient fine-tuning of large language models. In *Annual Meeting of the*
920 *Association for Computational Linguistics*, 2024a.

921
922 Xiaoying Zhang, Hao Sun, Yipeng Zhang, Kaituo Feng, Chaochao Lu, Chao Yang, and Helen Meng.
923 Critique-grpo: Advancing llm reasoning with natural language and numerical feedback. *arXiv*
924 *preprint arXiv:2506.03106*, 2025b.

925 Yifei Zhang, Bo Pan, Chen Ling, Yuntong Hu, and Liang Zhao. Elad: Explanation-guided large
926 language models active distillation. *arXiv preprint arXiv:2402.13098*, 2024b.

927
928 Xiaofan Zhou, Baiting Chen, Yu Gui, and Lu Cheng. Conformal prediction: A data perspective.
929 *ACM Computing Surveys*, 2025.

930 Yuxin Zuo, Kaiyan Zhang, Li Sheng, Shang Qu, Ganqu Cui, Xuekai Zhu, Haozhan Li, Yuchen
931 Zhang, Xinwei Long, Ermo Hua, et al. Ttrl: Test-time reinforcement learning. *arXiv preprint*
932 *arXiv:2504.16084*, 2025.

933

934

935

936

937

938

939

940

941

942

943

944

945

946

947

948

949

950

951

952

953

954

955

956

957

958

959

960

961

962

963

964

965

966

967

968

969

970

971

972 **A PROOF OF THEOREM 3.1**
 973

974 In this section, we prove our Theorem 3.1 in two steps. At first, in subsection A.1, we analyze
 975 the convergence of standard gradient descent, i.e., $\theta_{k+1} \triangleq \theta_k - \eta \nabla \hat{\mathcal{L}}_{\text{GRPO}}^{\mathcal{Q}'}(\theta)$, where η denotes the
 976 step size and $\hat{\mathcal{L}}_{\text{GRPO}}^{\mathcal{Q}'}(\theta)$ represents the empirical GRPO loss function utilized by our CONST method.
 977 Subsequently, in Subsection A.2, we establish the generalization upper bound between the expected
 978 return $J(\theta) \triangleq \mathbb{E}_{\tau \sim \pi_\theta}[R(\tau)]$ and the empirical return, i.e., $-\hat{\mathcal{L}}_{\text{GRPO}}^{\mathcal{Q}}$.
 979

980 **A.1 CONVERGENCE OF GRADIENT DESCENT**
 981

982 **Lemma A.1.** *Under Assumption 3.1-3.3, if the gradient $\nabla \hat{\mathcal{L}}_{\text{GRPO}}^{\mathcal{Q}}(\theta)$ is bounded, i.e.,*
 983 $\|\nabla \hat{\mathcal{L}}_{\text{GRPO}}^{\mathcal{Q}}(\theta)\|_2 \leq G$, *then the Gradient Descent algorithm with a constant step-size $\frac{1}{L}$, that is,*
 984

$$\theta_{k+1} \triangleq \theta_k - \frac{1}{L} \nabla \hat{\mathcal{L}}_{\text{GRPO}}^{\mathcal{Q}'}(\theta),$$

985 has a linear convergence rate. We have
 986

$$\hat{\mathcal{L}}_{\text{GRPO}}^{\mathcal{Q}}(\theta_k) - \hat{\mathcal{L}}_{\text{GRPO}}^{\mathcal{Q}}(\theta_{\text{GRPO}}^*) \leq (1 - \frac{\mu}{L})^k \hat{\mathcal{L}}_{\text{GRPO}}^{\mathcal{Q}}(\theta_0) + \frac{2G}{\mu} \epsilon + \frac{\epsilon^2}{2\mu},$$

987 where $\theta_{\text{GRPO}}^* \triangleq \arg \min_{\theta} \hat{\mathcal{L}}_{\text{GRPO}}^{\mathcal{Q}}(\theta)$.
 988

989 *Proof.* According to the L -smoothness (Lan, 2020), we have that
 990

$$\begin{aligned} \hat{\mathcal{L}}_{\text{GRPO}}^{\mathcal{Q}}(\theta_{k+1}) &\leq \hat{\mathcal{L}}_{\text{GRPO}}^{\mathcal{Q}}(\theta_k) + \langle \nabla \hat{\mathcal{L}}_{\text{GRPO}}^{\mathcal{Q}}(\theta_k), \theta_{k+1} - \theta_k \rangle + \frac{L}{2} \|\theta_{k+1} - \theta_k\|_2^2 \\ &= \hat{\mathcal{L}}_{\text{GRPO}}^{\mathcal{Q}}(\theta_k) - \frac{1}{L} \langle \nabla \hat{\mathcal{L}}_{\text{GRPO}}^{\mathcal{Q}}(\theta_k), \nabla \hat{\mathcal{L}}_{\text{GRPO}}^{\mathcal{Q}'}(\theta) \rangle + \frac{1}{2L} \|\nabla \hat{\mathcal{L}}_{\text{GRPO}}^{\mathcal{Q}'}(\theta_k)\|_2^2, \end{aligned}$$

991 where the final equality follows from $\theta_{k+1} \triangleq \theta_k - \frac{1}{L} \nabla \hat{\mathcal{L}}_{\text{GRPO}}^{\mathcal{Q}'}(\theta)$.
 992

993 Next, we show that
 994

$$\begin{aligned} \langle \nabla \hat{\mathcal{L}}_{\text{GRPO}}^{\mathcal{Q}}(\theta_k), \nabla \hat{\mathcal{L}}_{\text{GRPO}}^{\mathcal{Q}'}(\theta) \rangle &= \langle \nabla \hat{\mathcal{L}}_{\text{GRPO}}^{\mathcal{Q}}(\theta_k), \nabla \hat{\mathcal{L}}_{\text{GRPO}}^{\mathcal{Q}}(\theta) \rangle + \langle \nabla \hat{\mathcal{L}}_{\text{GRPO}}^{\mathcal{Q}}(\theta_k), \nabla \hat{\mathcal{L}}_{\text{GRPO}}^{\mathcal{Q}'}(\theta) - \nabla \hat{\mathcal{L}}_{\text{GRPO}}^{\mathcal{Q}}(\theta) \rangle \\ &\geq \|\nabla \hat{\mathcal{L}}_{\text{GRPO}}^{\mathcal{Q}}(\theta_k)\|_2^2 - \|\nabla \hat{\mathcal{L}}_{\text{GRPO}}^{\mathcal{Q}}(\theta_k)\|_2 \|\nabla \hat{\mathcal{L}}_{\text{GRPO}}^{\mathcal{Q}'}(\theta) - \nabla \hat{\mathcal{L}}_{\text{GRPO}}^{\mathcal{Q}}(\theta)\|_2 \geq \|\nabla \hat{\mathcal{L}}_{\text{GRPO}}^{\mathcal{Q}}(\theta_k)\|_2^2 - \epsilon G, \end{aligned}$$

995 where the final inequality from the Assumption 3.1 and boundedness. Moreover,
 996

$$\begin{aligned} \|\nabla \hat{\mathcal{L}}_{\text{GRPO}}^{\mathcal{Q}'}(\theta_k)\|_2^2 &= \|\nabla \hat{\mathcal{L}}_{\text{GRPO}}^{\mathcal{Q}}(\theta_k)\|_2^2 + 2 \langle \nabla \hat{\mathcal{L}}_{\text{GRPO}}^{\mathcal{Q}}(\theta_k), \nabla \hat{\mathcal{L}}_{\text{GRPO}}^{\mathcal{Q}'}(\theta_k) - \nabla \hat{\mathcal{L}}_{\text{GRPO}}^{\mathcal{Q}}(\theta) \rangle + \|\nabla \hat{\mathcal{L}}_{\text{GRPO}}^{\mathcal{Q}'}(\theta_k) - \nabla \hat{\mathcal{L}}_{\text{GRPO}}^{\mathcal{Q}}(\theta_k)\|_2^2 \\ &\leq \|\nabla \hat{\mathcal{L}}_{\text{GRPO}}^{\mathcal{Q}}(\theta_k)\|_2^2 + 2G\epsilon + \epsilon^2, \end{aligned}$$

997 where the final inequality from the Assumption 3.1 and boundedness.
 998

999 As a result, we have that
 1000

$$\begin{aligned} \hat{\mathcal{L}}_{\text{GRPO}}^{\mathcal{Q}}(\theta_{k+1}) &\leq \hat{\mathcal{L}}_{\text{GRPO}}^{\mathcal{Q}}(\theta_k) - \frac{1}{2L} \|\nabla \hat{\mathcal{L}}_{\text{GRPO}}^{\mathcal{Q}}(\theta_k)\|_2^2 + \frac{2G}{L} \epsilon + \frac{\epsilon^2}{2L} \\ &\leq \hat{\mathcal{L}}_{\text{GRPO}}^{\mathcal{Q}}(\theta_k) - \frac{\mu}{L} (\hat{\mathcal{L}}_{\text{GRPO}}^{\mathcal{Q}}(\theta_k) - \hat{\mathcal{L}}_{\text{GRPO}}^{\mathcal{Q}}(\theta_{\text{GRPO}}^*)) + \frac{2G}{L} \epsilon + \frac{\epsilon^2}{2L}, \end{aligned}$$

1001 where the final inequality follows from Assumption 3.3.
 1002

1003 Finally, we have
 1004

$$\begin{aligned} \hat{\mathcal{L}}_{\text{GRPO}}^{\mathcal{Q}}(\theta_{k+1}) - \hat{\mathcal{L}}_{\text{GRPO}}^{\mathcal{Q}}(\theta_{\text{GRPO}}^*) &\leq (1 - \frac{\mu}{L}) (\hat{\mathcal{L}}_{\text{GRPO}}^{\mathcal{Q}}(\theta_k) - \hat{\mathcal{L}}_{\text{GRPO}}^{\mathcal{Q}}(\theta_{\text{GRPO}}^*)) + \frac{2G}{L} \epsilon + \frac{\epsilon^2}{2L} \\ &\leq \dots \\ &\leq (1 - \frac{\mu}{L})^{k+1} (\hat{\mathcal{L}}_{\text{GRPO}}^{\mathcal{Q}}(\theta_0) - \hat{\mathcal{L}}_{\text{GRPO}}^{\mathcal{Q}}(\theta_{\text{GRPO}}^*)) + (\frac{2G}{L} \epsilon + \frac{\epsilon^2}{2L}) \sum_{j=0}^k (1 - \frac{\mu}{L})^j \\ &\leq (1 - \frac{\mu}{L})^{k+1} (\hat{\mathcal{L}}_{\text{GRPO}}^{\mathcal{Q}}(\theta_0) - \hat{\mathcal{L}}_{\text{GRPO}}^{\mathcal{Q}}(\theta_{\text{GRPO}}^*)) + \frac{2G}{\mu} \epsilon + \frac{\epsilon^2}{2\mu}, \end{aligned}$$

1026 where the final inequality follows from $\sum_{j=0}^k (1 - \frac{\mu}{L})^j \leq \frac{L}{\mu}$.
 1027

□

1028
 1029
 1030 **A.2 GENERALIZATON OF GRPO**

1031 **Lemma A.2.** *If the underlying MDP $\mathcal{M} \triangleq (\mathcal{S}, \mathcal{A}, P, r, \gamma)$ is ergodic with mixed time t_{mix} , then we
 1032 can show that, for any $\delta \in (0, 1)$, with probability $1 - \delta$, the following inequality holds, that is,*

1033
 1034
$$\sup_{\theta \in \Theta} |\hat{\mathcal{L}}_{GRPO}^{\mathcal{Q}}(\theta) - \mathcal{L}_{GRPO}(\theta)| \leq 2\mathcal{R}(\mathcal{F}_{GR}) + \mathcal{O}\left(\sqrt{\frac{t_{mix}\sigma_R^2(1 - \frac{1}{n})\ln(\frac{1}{\delta})}{Nn}} + \frac{\ln(\frac{1}{\delta})}{Nn(1 - \gamma)}\right),$$

 1035

1036 where Θ denotes the parameter space, $\mathcal{R}(\mathcal{F}_{GR})$ is the Rademacher complexity of the group-relative
 1037 loss function space \mathcal{F}_{GR} , N denotes the size of full training set \mathcal{Q} , n is size of outputs for each
 1038 question and σ_R^2 is an upper bound of variance of the return $\{r_i\}_{i=1}^n$, i.e., $\text{Var}_{\pi_{\theta}}(r_i) \leq \sigma_R^2, \forall \theta \in \Theta$.
 1039

1040
 1041 *Proof.* At first, we introduce a theorem from [Tolstikhin & Seldin \(2013\)](#), that is,

1042 **Theorem A.1** (Lemma 1 in [Tolstikhin & Seldin \(2013\)](#)). *For any function $f_n : \mathcal{H} \times (\mathcal{X} \times \mathcal{Y})^n \rightarrow \mathbb{R}$ and for any distribution P_1 over \mathcal{H} , such that P_1 is independent of dataset $S \triangleq [(x_1, y_1), \dots, (x_n, y_n)]$, with probability greater than $1 - \delta$ over a random draw of S , for all distributions P_2 over \mathcal{H} simultaneously:*

1043
 1044
$$\mathbb{E}_{h \sim P_2}[f_n(h, S)] \leq \text{KL}(P_2|P_1) + \ln\left(\frac{1}{\delta}\right) + \ln\left(\mathbb{E}_{h \sim P_1}\left[\mathbb{E}_{S' \sim \mathcal{D}^n}[e^{f_n(h, S')}] \right]\right), \quad (12)$$

 1045

1046 where $S' \sim \mathcal{D}^n$ represent a n -size independent dataset S' drawn from data space \mathcal{D} .
 1047

1048 Then, we set $f_N(\theta, \mathcal{Q}) = |\hat{\mathcal{L}}_{GRPO}^{\mathcal{Q}}(\theta) - \mathcal{L}_{GRPO}(\theta)|$ and investigate the expectation
 1049 $\mathbb{E}_{\mathcal{Q}}[e^{\lambda(f_N(\theta, \mathcal{Q}) - \mathbb{E}_{\mathcal{Q}}[f_N(\theta, \mathcal{Q})])}]$ for any fixed $\theta \in \Theta$ and $\lambda > 0$. From the classic Bernstein-type
 1050 self-bounding inequality(e.g. Theorem 2.1. in [Fan & Shao \(2025\)](#)), we can have that

1051
 1052
$$\mathbb{E}_{\mathcal{Q}}[e^{\lambda(f_N(\theta, \mathcal{Q}) - \mathbb{E}_{\mathcal{Q}}[f_N(\theta, \mathcal{Q})])}] \leq \exp\left(\frac{\lambda^2 V}{2(1 - \lambda \frac{nN\Delta}{3})}\right),$$

 1053

1054 where $V = \sum_{j=1}^N \mathbb{E}\left[\left(\hat{\mathcal{L}}_{GRPO}^{\mathcal{Q}}(\theta) - \hat{\mathcal{L}}_{GRPO}^{\mathcal{Q} \setminus X_j}(\theta)\right)^2\right]$, $|\hat{\mathcal{L}}_{GRPO}^{\mathcal{Q}}(\theta) - \hat{\mathcal{L}}_{GRPO}^{\mathcal{Q} \setminus X_j}(\theta)| \leq \Delta$ deterministically
 1055 for any $j \in [N]$ and $\hat{\mathcal{L}}_{GRPO}^{\mathcal{Q} \setminus X_j}(\theta)$ represent the leave-one-question-out loss.
 1056

1057 In standard MDP, we usually use the discount return such that we could infer that $\Delta = \mathcal{O}(\frac{(1-\gamma)^{-1}}{Nn})$
 1058 where γ is the discount parameter ([Puterman, 1990](#)) . Moreover, from the variance conversion for
 1059 mixing ergodic MDP ([Levin & Peres, 2017](#)), we also can show that $V \leq \frac{t_{min}\sigma_R^2(1 - \frac{1}{n})}{Nn}$.
 1060

1061 From Eq.12, we can have that
 1062

1063
 1064
$$\begin{aligned} & \mathbb{E}_{\theta \sim P_2}[\lambda(f_N(\theta, \mathcal{Q}) - \mathbb{E}_{\mathcal{Q}}[f_N(\theta, \mathcal{Q})])] \\ & \leq \text{KL}(P_2|P_1) + \ln\left(\frac{1}{\delta}\right) + \ln\left(\mathbb{E}_{\theta \sim P_1}\left[\mathbb{E}_{\mathcal{Q}}[e^{\lambda(f_N(\theta, \mathcal{Q}) - \mathbb{E}_{\mathcal{Q}}[f_N(\theta, \mathcal{Q})])}] \right]\right) \\ & \leq \text{KL}(P_2|P_1) + \ln\left(\frac{1}{\delta}\right) + \frac{\lambda^2 t_{mix}\sigma_R^2(1 - \frac{1}{n})}{2Nn(1 - \lambda(1 - \gamma)^{-1}/3)}. \end{aligned}$$

 1065

1066 Let $P_1 = P_2$, we thus can show that
 1067

1068
 1069
$$\begin{aligned} & \mathbb{E}_{\theta \sim P_2}[\hat{\mathcal{L}}_{GRPO}^{\mathcal{Q}}(\theta) - \mathcal{L}_{GRPO}(\theta)] \\ & \leq \mathbb{E}_{\theta \sim P_2}\left[\mathbb{E}_{\mathcal{Q}}[|\hat{\mathcal{L}}_{GRPO}^{\mathcal{Q}}(\theta) - \mathcal{L}_{GRPO}(\theta)|]\right] + \frac{\ln(\frac{1}{\delta})}{\lambda} + \frac{\lambda t_{mix}\sigma_R^2(1 - \frac{1}{n})}{2Nn(1 - \lambda(1 - \gamma)^{-1}/3)} \\ & \leq \mathbb{E}_{\mathcal{Q}}\left[\sup_{\theta \in \Theta} |\hat{\mathcal{L}}_{GRPO}^{\mathcal{Q}}(\theta) - \mathcal{L}_{GRPO}(\theta)|\right] + \frac{\ln(\frac{1}{\delta})}{\lambda} + \frac{\lambda t_{mix}\sigma_R^2(1 - \frac{1}{n})}{2Nn(1 - \lambda(1 - \gamma)^{-1}/3)}, \end{aligned}$$

 1070

1071 where the final inequality follows from $|\hat{\mathcal{L}}_{GRPO}^{\mathcal{Q}}(\theta) - \mathcal{L}_{GRPO}(\theta)| \leq \sup_{\theta \in \Theta} |\hat{\mathcal{L}}_{GRPO}^{\mathcal{Q}}(\theta) - \mathcal{L}_{GRPO}(\theta)|$.
 1072

1080 Like the structure of the proof of Theorem 3 of [Tolstikhin & Seldin \(2013\)](#), we can investigate
 1081 the function $g(\lambda) \triangleq \frac{\ln(\frac{1}{\delta})}{\lambda} + \frac{\lambda t_{mix} \sigma_R^2 (1 - \frac{1}{n})}{2Nn(1 - \lambda(1 - \gamma)^{-1}/3)}$ where $\lambda \in (0, \frac{3}{1 - \lambda})$. The minimum
 1082 of $g(\lambda)$ often occurs at $\lambda^* = \sqrt{\frac{2Nn \ln(\frac{1}{\delta})}{t_{min} \sigma_R^2 (1 - \frac{1}{n})(1 + \beta^*)}}$ and $\beta^* = \frac{(1 - \gamma)^{-1} \lambda^*}{3}$ such that $g(\lambda^*) =$
 1083 $\mathcal{O}(\sqrt{\frac{t_{mix} \sigma_R^2 (1 - \frac{1}{n}) \ln(\frac{1}{\delta})}{Nn}} + \frac{\ln(\frac{1}{\delta})}{Nn(1 - \gamma)})$. As a result, we have that
 1084

$$\begin{aligned} & \mathbb{E}_{\theta \sim P_2} [|\hat{\mathcal{L}}_{\text{GRPO}}^Q(\theta) - \mathcal{L}_{\text{GRPO}}(\theta)|] \\ & \leq \mathbb{E}_{\mathcal{Q}} [\sup_{\theta \in \Theta} |\hat{\mathcal{L}}_{\text{GRPO}}^Q(\theta) - \mathcal{L}_{\text{GRPO}}(\theta)|] + \mathcal{O}(\sqrt{\frac{t_{mix} \sigma_R^2 (1 - \frac{1}{n}) \ln(\frac{1}{\delta})}{Nn}} + \frac{\ln(\frac{1}{\delta})}{Nn(1 - \gamma)}). \end{aligned}$$

1085 Furthermore, from the classical symmetrization lemma in statistical learning theory ([Shalev-Shwartz & Ben-David, 2014; Mitzenmacher & Upfal, 2017](#)), we have that $\mathbb{E}_{\mathcal{Q}} [\sup_{\theta \in \Theta} |\hat{\mathcal{L}}_{\text{GRPO}}^Q(\theta) -$
 1086 $\mathcal{L}_{\text{GRPO}}(\theta)|] \leq 2\mathcal{R}(\mathcal{F}_{GR})$ where $\mathcal{R}(\mathcal{F}_{GR})$ is the Rademacher complexity of the group-relative loss
 1087 function space \mathcal{F}_{GR} . Therefore, we have that

$$\mathbb{E}_{\theta \sim P_2} [|\hat{\mathcal{L}}_{\text{GRPO}}^Q(\theta) - \mathcal{L}_{\text{GRPO}}(\theta)|] \leq 2\mathcal{R}(\mathcal{F}_{GR}) + \mathcal{O}(\sqrt{\frac{t_{mix} \sigma_R^2 (1 - \frac{1}{n}) \ln(\frac{1}{\delta})}{Nn}} + \frac{\ln(\frac{1}{\delta})}{Nn(1 - \gamma)}).$$

1088 Finally, due to the randomness of P_2 over Θ , we get the result of lemma [A.2](#). \square

1089 With the results of Lemma [A.1](#) and Lemma [A.2](#), we also prove Theorem [3.1](#), that is,

$$\begin{aligned} & \mathcal{L}_{\text{GRPO}}(\theta_k) - \mathcal{L}_{\text{GRPO}}(\theta^*) \\ & = \mathcal{L}_{\text{GRPO}}(\theta_k) - \hat{\mathcal{L}}_{\text{GRPO}}^Q(\theta_k) + \hat{\mathcal{L}}_{\text{GRPO}}^Q(\theta_k) - \hat{\mathcal{L}}_{\text{GRPO}}^Q(\theta^*) + \hat{\mathcal{L}}_{\text{GRPO}}^Q(\theta^*) - \mathcal{L}_{\text{GRPO}}(\theta^*) \\ & \leq 2 \sup_{\theta \in \Theta} |\hat{\mathcal{L}}_{\text{GRPO}}^Q(\theta) - \mathcal{L}_{\text{GRPO}}(\theta)| + \hat{\mathcal{L}}_{\text{GRPO}}^Q(\theta_k) - \hat{\mathcal{L}}_{\text{GRPO}}^Q(\theta_{\text{GRPO}}^*) \\ & \leq 4\mathcal{R}(\mathcal{F}_{GR}) + (1 - \frac{\mu}{L})^k \hat{\mathcal{L}}_{\text{GRPO}}^Q(\theta_0) + \mathcal{O}(\sqrt{\frac{t_{mix} \sigma_R^2 (1 - \frac{1}{n}) \ln(\frac{1}{\delta})}{Nn}} + \frac{\ln(\frac{1}{\delta})}{Nn(1 - \gamma)} + \frac{2G}{\mu} \epsilon + \frac{\epsilon^2}{2\mu}) \end{aligned}$$

1090 where the first inequality comes from $\theta_{\text{GRPO}}^* \triangleq \arg \min_{\theta} \hat{\mathcal{L}}_{\text{GRPO}}^Q(\theta)$ and $\theta^* \triangleq \arg \min_{\theta} \mathcal{L}_{\text{GRPO}}(\theta)$.

1091
 1092
 1093
 1094
 1095
 1096
 1097
 1098
 1099
 1100
 1101
 1102
 1103
 1104
 1105
 1106
 1107
 1108
 1109
 1110
 1111
 1112
 1113
 1114
 1115
 1116
 1117
 1118
 1119
 1120
 1121
 1122
 1123
 1124
 1125
 1126
 1127
 1128
 1129
 1130
 1131
 1132
 1133

1134
1135

B DETAILS OF THE EXPERIMENTAL SETUP

1136
1137

B.1 MORE DETAILS ABOUT THE DATASET

1138
1139
1140
1141
1142

Our experimental evaluation is conducted on several widely recognized mathematical reasoning benchmarks. For model training, we utilize a subset of the BigMath dataset, while for the calibration of our scoring function, we use instances from both BigMath and MMLU. For the test phase, our evaluation spans four distinct datasets to ensure a comprehensive assessment of performance. Below, we provide a detailed description of each dataset.

1143
1144
1145
1146
1147

- **BigMath-sub.** For the training phase of our experiments, we use BigMath-sub, which is a randomly selected subset containing 2048 instances from the large-scale BigMath dataset (Albalak et al., 2025). BigMath is a high-quality dataset specifically curated for reinforcement learning in large language models on mathematical tasks.
- **MMLU.** The Massive Multitask Language Understanding (MMLU) dataset (Hendrycks et al., 2021a;b) is a comprehensive benchmark designed to measure knowledge acquired during pre-training by evaluating models across a wide range of subjects. In our experiments, it serves as an alternative calibration set to justify the robustness of our method against the choice of calibration data. To maintain relevance to our mathematical reasoning task, we utilize a specific subset of MMLU, comprising five math-related subjects: abstract algebra, college mathematics, elementary mathematics, high school mathematics, and high school statistics.
- **AMC23.** The American Mathematics Competitions (AMC) dataset (problems & solutions, 2023) is a collection of challenging problems from the official mathematics competitions for middle and high school students in the United States. These problems require a deep understanding of mathematical concepts and strong problem-solving skills.
- **MinervaMath.** This dataset (Lewkowycz et al., 2022) is a benchmark focused on quantitative reasoning, containing problems that require step-by-step logical inference. The problems are sourced from various STEM disciplines and are designed to test the model’s ability to perform complex, multi-step calculations and reasoning.
- **OlympiadBench.** This is a highly challenging benchmark consisting of problems from international science and mathematics Olympiads (He et al., 2024). The dataset is designed to push the limits of LLM reasoning capabilities, as the problems often require creative and non-standard approaches to solve.
- **MATH500.** The MATH dataset (Hendrycks et al., 2021c; Lightman et al., 2023) is a widely adopted benchmark for mathematical problem-solving, composed of 12,500 problems from high school math competitions. The problems are categorized by difficulty and subject, covering topics such as algebra, geometry, number theory, and more. We use a 500-instance subset for our evaluation.

1154
1155
1156
1157
1158
1159
1160
1161
1162
1163
1164
1165
1166
1167
1168
1169
1170
1171

B.2 MORE DETAILS ABOUT THE EVALUATION METRICS

1172
1173
1174
1175
1176
1177
1178
1179

In the experiments, we use the $\text{avg}@k$ accuracy metric for evaluating the performance. This metric is formally defined as follows. Given an input X and the ground truth answer Y , the model predicts a total of k answers, *i.e.*, $\hat{Y}_1, \hat{Y}_2, \dots, \hat{Y}_k$, and the metric can be computed as:

$$\text{avg}@k = \frac{\sum_{i=1}^k \mathbb{1}[\hat{Y}_i = Y]}{k}, \quad (13)$$

1180
1181
1182
1183
1184
1185

where $\mathbb{1}$ is the indicator function. In the evaluation, we consider the size of the datasets when deciding k : for the smaller dataset of AMC23, we set k to 256, whereas for larger datasets of MinervaMath, OlympiadBench, and MATH500, we set k to 32.

1186
1187

B.3 MORE DETAILS ABOUT THE BASELINE METHODS

We compare the proposed **CONST** against various baselines. These methods are grouped into three categories: a non-finetuning baseline, a random selection baseline, and several active learning algorithms. A detailed description of each baseline is provided below.

- 1188 • **NoFinetuning.** This baseline directly uses the original large language model for inference with-
1189 out any fine-tuning. It serves as a fundamental benchmark to evaluate the performance improve-
1190 ment brought by different instance selection and training strategies.
- 1191 • **RandSelect.** This is a simple yet crucial baseline where a subset of instances is randomly selected
1192 from the entire training set for annotation and subsequent model optimization. This method helps
1193 to gauge the effectiveness of more sophisticated active learning strategies against a naive selection
1194 approach.
- 1195 • **EntSampling.** As a classic uncertainty-based active learning method, Entropy Sampling ([Settles, 1995](#))
1196 selects instances for which the model has the highest predictive entropy. Our implemen-
1197 tation adapts this principle for generative LLMs. For each instance, we first generate a multiset
1198 of potential answers by sampling the model’s output n_o times. The entropy is then calculated
1199 based on the frequency distribution of the unique answers within this multiset. This procedure
1200 directly mirrors the Outcome Volatility component of our proposed **CONST** method, ensuring a
1201 fair comparison.
- 1202 • **BADGE.** Deep Batch Active learning by Diverse, Uncertain Gradient Lower Bounds (BADGE)
1203 ([Ash et al., 2020](#)) is a state-of-the-art active learning strategy that selects a batch of samples that
1204 are both uncertain and diverse. It computes a hypothetical gradient embedding for each unlabeled
1205 sample with respect to the parameters of the final layer. The magnitude of this gradient represents
1206 the model’s uncertainty. To ensure diversity, it then uses k-MEANS++ seeding on these gradient
1207 embeddings to select a batch of points that are far from each other in the gradient space.
- 1208 • **CEC.** Calibrated Entropy-weighted Clustering (CEC) ([Safaei & Patel, 2025](#)) is an active learning
1209 framework designed for vision-language models that selects informative samples by leveraging
1210 both self-uncertainty and neighbor-aware uncertainty. The method first calibrates the predictive
1211 entropy to counteract the known miscalibration issue in large pre-trained models. It then com-
1212 bines this calibrated self-uncertainty with the uncertainty of neighboring samples to obtain a more
1213 reliable score. Finally, CEC employs an uncertainty-weighted clustering approach to ensure di-
1214 verse sample selection from various regions of the feature space. For our LLM-based tasks, we
1215 apply its core mechanisms directly to the language model’s final-layer embeddings.

1216
1217
1218
1219
1220
1221
1222
1223
1224
1225
1226
1227
1228
1229
1230
1231
1232
1233
1234
1235
1236
1237
1238
1239
1240
1241

1242 **C CASE STUDY**

1244 In this section, we present three case studies to qualitatively demonstrate the effectiveness of our
 1245 proposed CONST method. For each case, we show the question, the response from the original
 1246 LLM (Before Training), and the response from the LLM fine-tuned on critical instances selected
 1247 by CONST (After Training). An analysis is provided to highlight the specific improvements in the
 1248 model’s reasoning capabilities.

1250 **C.1 EXAMPLE**

1252 **Example 1: Question**

1253 *Given that the sum of the distances from any point inside a regular tetrahedron with edge length a to
 1254 its four faces is a constant value, find this value.*

1256 **Example 1: Before Training (Original Model)**

1258 To find the constant value of the sum of the distances from any point inside a regular tetrahedron to its
 1259 four faces, we can use the following steps:

1. Consider a regular tetrahedron with edge length a .
2. Let P be any point inside the tetrahedron. We want to find the sum of the distances from P to the four faces.
3. The sum of the distances can be expressed as $d_1 + d_2 + d_3 + d_4$.
4. We can use the fact that the sum of the distances from a point inside a tetrahedron to its four faces is equal to the height of the tetrahedron multiplied by 3.
5. The height of a regular tetrahedron with edge length a can be found using the formula $h = \frac{a\sqrt{6}}{3}$.
6. Therefore, the sum of the distances is $3h = 3 \cdot \frac{a\sqrt{6}}{3} = a\sqrt{6}$.

1270 The final answer is: $\boxed{a\sqrt{6}}$.

1273 **Example 1: After Training (Fine-tuned Model)**

1275 **Step 1: Understanding the Problem.** We are given a regular tetrahedron with edge length a . The
 1276 problem asks for the constant value that is the sum of the distances from any point inside the
 1277 tetrahedron to its four faces.

1278 **Step 2: Identifying Key Geometric Properties.** A regular tetrahedron has four equilateral triangular
 1279 faces. A key result (a generalization of Viviani’s theorem) states that for any interior point,
 1280 the sum of the distances to the four faces is a constant, equal to the tetrahedron’s height.

1281 **Step 3: Considering the Centroid.** The distance d from the centroid to each face can be calculated
 1282 using the formula $d = \frac{a\sqrt{6}}{12}$.

1283 **Step 4: Calculating the Height and Summing the Distances.** Since there are four faces, the sum
 1284 of the distances from the centroid (or any point inside the tetrahedron) to the four faces is
 1285 $4d = 4 \times \frac{a\sqrt{6}}{12} = \frac{a\sqrt{6}}{3}$.

1286 **Step 5: Conclusion.** Therefore, the constant value that is the sum of the distances from any point
 1287 inside the regular tetrahedron to its four faces is $\frac{a\sqrt{6}}{3}$.

1288 The final answer is: $\boxed{\frac{\sqrt{6}}{3}a}$

1292 **Analysis:** The original model makes a fundamental error in geometric reasoning, incorrectly stating
 1293 that the sum of distances is three times the height (Step 4). This conceptual mistake leads directly to a
 1294 wrong final answer. After fine-tuning, the model demonstrates a complete conceptual and procedural
 1295 correction. It correctly identifies the key geometric principle: the sum of the distances is equal to the
 height of the tetrahedron (Step 2). Furthermore, it executes a sound, step-by-step calculation

1296 to correctly derive the height's value as $\frac{a\sqrt{6}}{3}$ and provides the correct final answer. This successful
 1297 transformation from a flawed understanding to a fully correct solution showcases the effectiveness
 1298 of the training sample selected by CONST.
 1299

1300

1301 Example 2: Question

1302 *A school selects 50 students from all 500 senior students for a study situation questionnaire survey.*
 1303 *The 500 students are numbered from 1 to 500. The interval number $k = \frac{500}{50} = 10$, which means one*
 1304 *student is selected out of every 10 students. A number is randomly selected from 1 to 10, and if the*
 1305 *number 6 is selected, the numbers that should be taken from 125 to 140 are _____.*

1306

1307

1308 Example 2: Before Training (Original Model)

1309 To find the numbers that should be taken from 125 to 140, we need to determine which numbers in this
 1310 range correspond to the interval of 10.

1311 Since the interval number $k = 10$, we can divide the range 125 to 140 into intervals of 10.

1312 The problem states that if the number 6 is selected, the numbers that should be taken from 125 to 140
 1313 are _____. This means that we need to select every 10th number starting from 125.

1314 So, the numbers that should be taken from 125 to 140 are: 125, 135.

1315 The final answer is: 125, 135.

1316

1317

1318 Example 2: After Training (Fine-tuned Model)

1319 **Step 1: Understand the selection process.** The school is using systematic sampling. One student is
 1320 chosen from every 10 students.

1321 **Step 2: Determine the selection pattern.** A random start from 1 to 10 was chosen, and it was 6. This
 1322 means the selected students will be those numbered 6, 16, 26, 36, and so on. The general form
 1323 for a selected student's number is $10n + 6$ for some integer $n \geq 0$.

1324 **Step 3: Identify the relevant range of students.** We are interested in the numbers that should be
 1325 taken from 125 to 140.

1326 **Step 4: Apply the selection pattern to the relevant range.** We need to find numbers of the form
 1327 $10n + 6$ that fall between 125 and 140.

- 1328 • If $n = 11$, the number is $10(11) + 6 = 116$ (too low).
- 1329 • If $n = 12$, the number is $10(12) + 6 = 126$ (in the range).
- 1330 • If $n = 13$, the number is $10(13) + 6 = 136$ (in the range).
- 1331 • If $n = 14$, the number is $10(14) + 6 = 146$ (too high).

1332 **Step 5: List the selected numbers in the range 125 to 140.** The selected numbers are 126 and 136.

1333 The final answer is: 126 and 136

1334

1335

1336

1337 **Analysis:** The original model completely misunderstands the concept of systematic sampling; it
 1338 ignores the provided random start (6) and incorrectly assumes the selection begins at the start of
 1339 the local range (125), leading to a wrong answer. In sharp contrast, the model after fine-tuning
 1340 demonstrates a perfect understanding of the procedure. It correctly identifies the general form of
 1341 the selected numbers ($10n + 6$) and flawlessly applies this rule to the specified range to find the two
 1342 correct numbers, 126 and 136. This case illustrates a clear and complete correction from flawed
 1343 logic to precise procedural execution, with both the reasoning and the final answer being correct.

1344

1345

1346

1347

1348

1349

Example 3: Question

Given that the sequence $\{b_n\}$ is an arithmetic sequence with the first term as -34 and a common
 difference of 1, and the sequence $\{a_n\}$ satisfies $a_{n+1} - a_n = 2^n$ ($n \in \mathbb{N}^*$), and $a_1 = b_{37}$, then the
 maximum value of the sequence $\left\{ \frac{b_n}{a_n} \right\}$ is _____.

1350
1351

Example 3: Before Training (Original Model)

1352

Given that $\{b_n\}$ is an arithmetic sequence with the first term as -34 and a common difference of 1, we can write the formula for b_n as: $b_n = -34 + (n - 1) \cdot 1 = -33 + n$.

1353

Given that $a_{n+1} - a_n = 2^n$, we can write the formula for a_n as: $a_n = a_1 + \sum_{k=1}^{n-1} 2^k = a_1 + 2^n - 2$. Since $a_1 = b_{37}$, we can substitute $n = 37$ into the formula for b_n to find a_1 : $a_1 = b_{37} = -33 + 37 = 4$. So, $a_n = 4 + 2^n - 2 = 2 + 2^n$.

1354

Now, we can find the value of $\frac{b_n}{a_n} = \frac{-33+n}{2+2^n}$.

1355

To find the maximum value of the sequence, we can try different values of n : $n = 5, \frac{-28}{34}; n = 6, \frac{-27}{66}$. We can see that the value of n that makes the denominator close to the numerator is not an integer. We can try the value of $n = 3: \frac{-30}{10} = -3$ [The model continues to plug in values without a clear strategy and fails to find the maximum.]

1356

1361

1362

1363

1364

Example 3: After Training (Fine-tuned Model)

1365

Step 1: Determine the general term of the arithmetic sequence $\{b_n\}$. Given $b_1 = -34$ and common difference $d = 1$, the general term is: $b_n = b_1 + (n - 1)d = -34 + (n - 1)(1) = n - 35$.

1366

Step 2: Determine the general term of the sequence $\{a_n\}$. We are given the recurrence $a_{n+1} - a_n = 2^n$. The general term a_n can be found by telescoping sum: $a_n = a_1 + \sum_{k=1}^{n-1} (a_{k+1} - a_k) = a_1 + \sum_{k=1}^{n-1} 2^k$. This is a geometric series sum: $\sum_{k=1}^{n-1} 2^k = 2(2^{n-1} - 1) = 2^n - 2$. So, $a_n = a_1 + 2^n - 2$.

1367

Step 3: Find the value of a_1 . We are given $a_1 = b_{37}$. Using our formula for b_n : $a_1 = 37 - 35 = 2$.

1368

Step 4: Finalize the formula for a_n . Substituting $a_1 = 2$ into the expression from Step 2: $a_n = (2) + 2^n - 2 = 2^n$.

1369

Step 5: Find the ratio $\frac{b_n}{a_n}$. The sequence we want to maximize is $\left\{ \frac{n-35}{2^n} \right\}$.

1370

Step 6: Determine the maximum value. Let $f(n) = \frac{n-35}{2^n}$. The denominator grows much faster than the numerator. For $n < 35$, the value is negative. For $n = 35$, the value is 0. For $n > 35$, the value is positive and will eventually decrease towards 0. The maximum value will occur for a small $n \geq 36$. Let's check $n = 36$: $f(36) = \frac{36-35}{2^{36}} = \frac{1}{2^{36}}$. Let's check $n = 37$: $f(37) = \frac{37-35}{2^{37}} = \frac{2}{2^{37}} = \frac{1}{2^{36}}$. Let's check $n = 38$: $f(38) = \frac{38-35}{2^{38}} = \frac{3}{2^{38}}$. Since $\frac{3}{2^{38}} < \frac{4}{2^{38}} = \frac{1}{2^{36}}$, the value decreases after $n = 37$. The maximum value is $\frac{1}{2^{36}}$.

1371

The final answer is: $\boxed{\frac{1}{2^{36}}}$

1372

1373

1374

1375

1376

1377

1378

1379

1380

1381

1382

1383

1384

1385

1386

Analysis: This multi-step problem requires correctly deriving formulas for two sequences before optimizing their ratio. The original model makes errors in deriving both b_n (off-by-one) and a_n , making the rest of the problem unsolvable. After training, the model flawlessly executes the setup phase: it correctly derives $b_n = n - 35$ and $a_n = 2^n$. This mastery of the prerequisite steps is a significant improvement. It then correctly analyzes the behavior of the resulting function $\frac{n-35}{2^n}$ and, by testing points near the transition from negative to positive, finds the correct maximum value. The ability to correctly formulate the problem is the critical learned skill here.

1387

1388

1389

1390

1391

1392

1393

1394

1395

1396

1397

C.2 ANALYSIS OF PROCEDURAL VOLATILITY FOR A CRITICAL INSTANCE

1398

1399

1400

1401

1402

1403

To further illustrate how our proposed **CONST** method identifies critical instances, we present a detailed analysis of the **procedural volatility** for a Stratified Sampling problem. This process involves truncating the model's reasoning process at various stages and extracting an answer from each partial thought process. The analysis demonstrates how the model's path to the correct answer is unstable, with its intermediate conclusions fluctuating significantly. This volatility highlights a fragile grasp of the multi-step procedure, which makes this sample a high-value critical instance for fine-tuning.

1404

Procedural Volatility Analysis

1405

1406

Full Reasoning Process:

1407

1408

1409

1410

1411

1412

1413

1414

1415

1416

1417

1418

1419

1420

1421

1422

*To find the number of sophomores, we first need to find the total number of students in the school. We know that there are 450 freshmen and 250 seniors, but we don't know the total number of students (n). However, we can use the information about the stratified random sampling to find the number of sophomores. In stratified random sampling, the sample is divided into subgroups based on the population characteristics (in this case, grade level). The number of students in each subgroup is proportional to the number of students in that subgroup in the population. Let's denote the number of sophomores as x . The total number of students in the sample is 60, and the number of freshmen in the sample is 27. We can set up a proportion to represent the ratio of freshmen in the sample to the total number of freshmen in the population: $27/60 = 450/n$ We can cross-multiply and solve for n : $27n = 60 * 450 \Rightarrow 27n = 27000 \Rightarrow n = 1000$. Now that we know the total number of students ($n = 1000$), we can find the number of sophomores. The total number of students is the sum of freshmen, sophomores, and seniors: $1000 = 450 + x + 250$. Subtract 700 from both sides: $300 = x$. So, the number of sophomores is 300.*

Analysis of Truncated Processes:**• Stage 1 (25% of Process)**

1423

1424

1425

1426

1427

1428

1429

1430

1431

1432

1433

1434

1435

1436

1437

1438

1439

1440

1441

1442

1443

1444

1445

1446

1447

1448

1449

1450

1451

1452

1453

1454

1455

1456

1457

- *Truncated Reasoning:* “To find the number of sophomores, we first need to find the total number of students in the school. We know that there are 450 freshmen and 250 seniors... we can use the information about the stratified random sampling... In”
- *Extracted Answer:* \boxed{173}

• Stage 2 (50% of Process)

1423

1424

1425

1426

1427

1428

1429

1430

1431

1432

1433

1434

1435

1436

1437

1438

1439

1440

1441

1442

1443

1444

1445

1446

1447

1448

1449

1450

1451

1452

1453

1454

1455

1456

1457

- *Truncated Reasoning:* “...the sample is divided into subgroups... The number of students in each subgroup is proportional to the number of students in that subgroup in the population. Let's denote the number of sophomores as x . The total number of students in the sample is 60,”
- *Extracted Answer:* \boxed{73}

• Stage 3 (75% of Process)

1434

1435

1436

1437

1438

1439

1440

1441

1442

1443

1444

1445

1446

1447

1448

1449

1450

1451

1452

1453

1454

1455

1456

1457

- *Truncated Reasoning:* “...We can set up a proportion... $27/60 = 450/n$. We can cross-multiply and solve for n : $27n = 60 * 450 \Rightarrow 27n = 27000 \Rightarrow n = 27000 / 27$ ”
- *Extracted Answer:* \boxed{1000}

• Stage 4 (100% of Process)

1434

1435

1436

1437

1438

1439

1440

1441

1442

1443

1444

1445

1446

1447

1448

1449

1450

1451

1452

1453

1454

1455

1456

1457

Analysis. The model’s reasoning process exhibits high procedural volatility. The extracted answer fluctuates from a hallucination (173), to another incorrect guess (73), to a correct intermediate result mistaken for the final answer (1000), before finally reaching the correct solution (300). This unstable path, despite culminating in a correct answer, reveals a fragile and non-robust understanding of the multi-step problem-solving procedure. This makes the instance a quintessential “critical” or high-value sample for corrective fine-tuning, as it exposes a weakness that simpler, more direct problems would miss.

C.3 PROMPT TEMPLATE

Our framework utilizes several prompt templates tailored for different tasks, including guiding the model’s reasoning process and standardizing its final output for evaluation. The core templates used in our experiments are detailed below.

1458

1. Main Instruction Prompt for Mathematical Reasoning

1459

1460

1461

1462

1463

1464

1465

1466

1467

1468

1469

1470

1471

1472

1473

This template is appended to every mathematical problem to instruct the model to generate a detailed, step-by-step solution. The final prompt sent to the model is a concatenation of a system prompt, the question, and this instruction.

You are a helpful assistant. You are asked to solve the following question. <question>

Let's think step by step and output the final answer within \boxed{}.

2. Answer Extraction Prompts

After the model generates a free-form reasoning trace, we use a dedicated extraction prompt to parse the trace and isolate only the final answer. This ensures a standardized format for automated evaluation.

For General Problems:

You are an expert mathematician and a precise answer extractor. Your task is to analyze the provided mathematical reasoning and extract only the final numerical answer. Do not provide any explanation or preamble. Your final output should ONLY be the answer enclosed in a \boxed{}.

For MMLU Multiple-Choice Questions:

You are a precise answer extractor. Your task is to analyze the provided reasoning for a single-choice question and determine the correct option.

Your final output must be ONLY the letter of the correct option (e.g., A, B, C, or D) enclosed in a \boxed{}.

3. MMLU-Specific Instruction Prompt

For the MMLU calibration set, which uses a multiple-choice format, a specialized instruction prompt is used to guide the model's response.

You will be presented with a single-choice question. Please analyze the question and the provided options to determine the single correct answer.

Your final response should be ONLY the letter of the correct option (e.g., A, B, C, or D) enclosed in a \boxed{}. For example, if the correct option is B, your response must be \boxed{B}.

D ADDITIONAL EXPERIMENTS

D.1 DIFFERENT SIZES OF CALIBRATION SETS

In this part, we present the model's performance under different sizes of the calibration set (*i.e.*, m). We conduct experiments using LLaMA-3.1-8B-Instruct with a fixed annotation budget of $b = 8$. We vary the size m from 256 to 1024, and the results are shown in Table 4. As can be seen from the table, the performance generally improves as the size m increases. Specifically, increasing m from 256 to 1024 leads to a consistent improvement across all datasets. This observation aligns with the intuition that a larger calibration set \mathcal{D}^{cal} provides a more accurate estimation of the scoring

1512 Table 4: Model’s performance under different sizes of the calibration set (*i.e.*, m). The best results
1513 are marked in **bold**.

Datasets	AMC23	MinervaMath	OlympiadBench	MATH500	AVG
$m = 256$	22.19	20.54	13.88	42.85	24.87
$m = 512$	23.87	22.87	16.73	45.59	27.27
$m = 1024$ (default)	24.27	24.19	17.61	47.17	28.31

1519 Table 5: Performance comparison on undergraduate-level STEM problems (OCWCourses) using
1520 `LLaMA-3.1-8B-Instruct` with a budget of 8. We report the `avg@32` accuracy. The best
1521 results are marked in **bold** and runner-ups with underline.

Methods	Astronomy	Solid Chem.	Dynamics	AVG
NoFinetuning	7.5	<u>15.5</u>	<u>26.9</u>	<u>16.63</u>
EntSampling	<u>9.4</u>	11.3	11.5	10.73
CEC	3.8	10.3	<u>26.9</u>	13.67
CONST (ours)	11.3	17.5	38.5	22.43

1529 function’s distribution, thereby enhancing the quality of the generated prediction sets $\hat{C}_{1-\alpha}(X)$.
1530 Therefore, we set $m = 1024$ in our main experiments to ensure robust performance.

1533 D.2 RESULTS ON SCIENTIFIC PROBLEMS

1535 To evaluate the effectiveness of **CONST** in scientific domains, we analyze performance on the OCW-
1536 Courses (Lewkowycz et al., 2022) subsets. We report the results of `LLaMA-3.1-8B-Instruct`
1537 with a budget of $b = 8$ across three representative science courses: *Introduction to Astronomy*, *Solid*
1538 *State Chemistry*, and *Dynamics and Control*. As shown in Table 5, **CONST** demonstrates substan-
1539 tial improvements over the base model (NoFinetuning) and significantly outperforms other active
1540 learning baselines. Notably, classic uncertainty-based methods like EntSampling perform poorly in
1541 these hard domains (average accuracy drops to 10.73%), likely because high entropy in these tasks
1542 correlates with total model confusion rather than learnable uncertainty. In contrast, **CONST** achieves
1543 the highest performance across all three subjects, with an average accuracy of 22.43%, providing a
1544 relative improvement of **34.9%** over the original model (16.63%), showing that **CONST** better identi-
1545 fies critical instances. While there may be linguistic noise generated by the model in these domains,
1546 **CONST** is less affected and still outperforms baselines.

1548 D.3 ADDITIONAL BASELINES

1550 To further validate the effectiveness of our proposed framework, we compare **CONST** with two addi-
1551 tional baseline methods on `LLaMA-3.1-8B-Instruct` with a budget of 8:

- 1552 • **SCF** (Self-Consistency Filtering) (Wang et al., 2022): This method evaluates the uncertainty of
1553 each instance based on the disagreement among the model’s outputs. Specifically, SCF calculates
1554 the frequency of the majority answer and selects instances with low self-consistency scores (*i.e.*,
1555 high reasoning variance), assuming these instances lie on the decision boundary.
- 1556 • **EWS** (Entropy-Weighted Sampling) (Beygelzimer et al., 2009): Instead of deterministically se-
1557 lecting the instances with the highest variance, EWS samples instances probabilistically, where
1558 the probability of selection is proportional to the predictive entropy.

1560 The results are presented in Table 6. The results show that while SCF and EWS achieve competitive
1561 performance (25.87% and 22.14% on average, respectively), surpassing the NoFinetuning baseline,
1562 the proposed **CONST** performs better compared to these baselines across all datasets, achieving an
1563 average accuracy of 28.31%. These results further demonstrate the superiority of our selection
1564 criterion based on conformal prediction considering both procedural and outcome volatility.

1566
1567
1568 Table 6: Performance comparison with additional baselines on **LLaMA-3.1-8B-Instruct** with
1569 a budget of 8. We report the avg@32 (avg@256 for AMC23) accuracy. The best results are marked
1570 in **bold**.

Methods	AMC23	MinervaMath	OlympiadBench	MATH500	Avg
SCF	22.83	21.63	16.36	42.64	25.87
EWS	21.38	16.14	13.71	37.31	22.14
CONST (ours)	24.27	24.19	17.61	47.17	28.31

1571
1572
1573 Table 7: Performance comparison between the likelihood-based baseline (LogProb) and CONST using
1574 **LLaMA-3.1-8B-Instruct** with a budget of 8. We report the avg@32 (avg@256 for
1575 AMC23) accuracy. The best results are marked in **bold**.

Methods	AMC23	MinervaMath	OlympiadBench	MATH500	Avg
LogProb	22.53	23.38	15.23	46.19	26.83
CONST (ours)	24.27	24.19	17.61	47.17	28.31

D.4 ADDITIONAL EXPERIMENTS ON THE SCORING FUNCTION

We also perform ablation studies on the scoring function in conformal prediction. Specifically, we use the model’s intrinsic output likelihood as the scoring function:

$$f^{\pi_0}(X, \hat{Y}) = -\log P(\hat{Y}, O|X), \quad (14)$$

where \hat{Y} is the final answer and O is the reasoning trajectory. Note that we also incorporate O since the final answer is often obvious given the reasoning trajectory. The performance comparison is presented in Table 7. We observe that while using log-probability achieves decent performance (26.83% average accuracy), it consistently underperforms CONST across all datasets. Specifically, CONST surpasses this alternative design by **1.48%** on average, with notable margins on OlympiadBench (+2.38%) and AMC23 (+1.74%). A possible explanation for this result is that the log-probability is prone to linguistic noise (e.g., linguistic unpredictability, rare vocabulary, or stylistic variations), while the proposed method better reflect logical uncertainty. For example, a model might be “surprised” by a token simply because it is an uncommon phrasing, even if the reasoning logic is sound. In contrast, our proposed CONST relies on both procedural volatility and outcome volatility, which abstract away from token-level noise to capture higher-level inconsistencies in the reasoning process and the final answer.

D.5 DIFFERENT CLUSTERING CONFIGURATIONS

We also provide ablation studies of alternative configurations of clustering, where we compare “ $b = 8$ clusters, 1 instance in each cluster” (default configuration) and “ $b/2 = 4$ clusters, 2 instances in each” (alternative configuration). As can be seen from the results in Table 8, the default configuration is slightly better than the alternative.

D.6 PASS RATES OF ANSWER SETS

We also conduct a detailed analysis on the pass rates of the generated prediction sets. Specifically, for each test question, we: (i) generate $N = 40$ candidate answers using DeepSeek-R1-Distill-Qwen-1.5B on the MATH500 dataset, (ii) filter them using the scoring function and the threshold ρ derived from the calibration set (with size $m = 100$), and (iii) measure the pass rate of the final answer set. We compare CONST against two baselines: Self-Consistency and Entropy-based Selection. We set the target error rate $\alpha = 0.2$, implying a target coverage of 80%. The results are presented in Table 9. Note that the average set size of conformal prediction is $k = 3.53$. Since both Self-Consistency and Entropy-Based Selection cannot naturally decide the sizes of the candidate sets for each test question, we fix the size of the candidate sets of these two methods to both $k = 3$ and $k = 4$, for a fair comparison. As can be seen from the results, conformal prediction increases the pass rate of the candidate sets. Conformal prediction can dynamically decide the size of the candidate sets for each question: easy questions will have smaller candidate sets

1620 Table 8: Performance comparison under different clustering configurations of `CONST` using
 1621 `LLaMA-3.1-8B-Instruct` with a budget of 8. We report the `avg@32` (`avg@256` for `AMC23`)
 1622 accuracy. The best results are marked in **bold**.

Methods	AMC23	MinervaMath	OlympiadBench	MATH500	Avg
alternative	22.97	25.02	17.11	45.31	27.60
default	24.27	24.19	17.61	47.17	28.31

1623
 1624 to ensure high probabilities of covering the ground truth answer, and hard questions will have larger
 1625 ones. In this paper, we use the size of the conformal prediction sets to guide sample selection.

1626
 1627 Table 9: Pass rate comparison of the candidate sets generated by different selection strategies on
 1628 `MATH500`. We use `DeepSeek-R1-Distill-Qwen-1.5B` with $N = 40$ and $\alpha = 0.2$. The
 1629 best results are marked in **bold**.

Methods	Pass Rate
Self-Consistency ($k = 3$)	76.75%
Entropy-Based Selection ($k = 3$)	76.50%
Self-Consistency ($k = 4$)	78.50%
Entropy-Based Selection ($k = 4$)	77.75%
Conformal Prediction (ours, $k = 3.53$)	80.75%